

Stony coral tissue loss disease intervention with amoxicillin leads to a reversal of disease-modulated gene expression pathways

Michael S. Studivan^{1,2,3}  | Ryan J. Eckert¹  | Erin Shilling¹  | Nash Soderberg^{2,3} 
 Ian C. Enochs³  | Joshua D. Voss¹ 

¹Harbor Branch Oceanographic Institute, Florida Atlantic University, Fort Pierce, Florida, USA

²University of Miami, Cooperative Institute for Marine and Atmospheric Studies, Miami, Florida, USA

³Ocean Chemistry and Ecosystems Division, NOAA Atlantic Oceanographic and Meteorological Laboratory, Miami, Florida, USA

Correspondence

Michael S. Studivan, University of Miami, Cooperative Institute for Marine and Atmospheric Studies, Miami, Florida, USA
 Email: studivanms@gmail.com

Present address

Erin Shilling, Department of Biology, Texas State University, San Marcos, Texas, USA

Funding information

Florida Department of Environmental Protection, Grant/Award Number: B55008; NOAA Coral Reef Conservation Program, Grant/Award Number: 31252; NOAA OAR 'Omics

Handling Editor: Pim Bongaerts

Abstract

Stony coral tissue loss disease (SCTLD) remains an unprecedented disease outbreak due to its high mortality rate and rapid spread throughout Florida's Coral Reef and wider Caribbean. A collaborative effort is underway to evaluate strategies that mitigate the spread of SCTLD across coral colonies and reefs, including restoration of disease-resistant genotypes, genetic rescue, and disease intervention with therapeutics. We conducted an in-situ experiment in Southeast Florida to assess molecular responses among SCTLD-affected *Montastraea cavernosa* pre- and post-application of the most widely used intervention method, CoreRx Base 2B with amoxicillin. Through Tag-Seq gene expression profiling of apparently healthy, diseased, and treated corals, we identified modulation of metabolomic and immune gene pathways following antibiotic treatment. In a complementary ex-situ disease challenge experiment, we exposed nursery-cultured *M. cavernosa* and *Orbicella faveolata* fragments to SCTLD-affected donor corals to compare transcriptomic profiles among clonal individuals from unexposed controls, those exposed and displaying disease signs, and corals exposed and not displaying disease signs. Suppression of metabolic functional groups and activation of stress gene pathways as a result of SCTLD exposure were apparent in both species. Amoxicillin treatment led to a 'reversal' of the majority of gene pathways implicated in disease response, suggesting potential recovery of corals following antibiotic application. In addition to increasing our understanding of molecular responses to SCTLD, we provide resource managers with transcriptomic evidence that disease intervention with antibiotics appears to be successful and may help to modulate coral immune responses to SCTLD. These results contribute to feasibility assessments of intervention efforts following disease outbreaks and improved predictions of coral reef health across the wider Caribbean.

KEY WORDS

antibiotic treatment, coral disease, disease transmission, Florida's Coral Reef, SCTLD, Tag-Seq, transcriptomics

1 | INTRODUCTION

Since its first observation near Miami, Florida in 2014, stony coral tissue loss disease (SCTLD) has spread throughout Florida's Coral Reef and to at least 25 jurisdictions across the wider Caribbean (Kramer et al., 2019; NOAA, 2018; Precht et al., 2016). The disease affects at least 24 scleractinian species and is characterized by subacute to acute tissue loss leading to colony mortality, often with formation of rapidly-progressing focal or multifocal lesions (Aeby et al., 2019, 2021) that are histologically distinct from white plague disease (Landsberg et al., 2020; NOAA, 2018). Histopathology has determined that tissue necrosis begins in the coral gastrodermis before progressing to the epithelial layer as a pale or bleached lesion (Aeby et al., 2019; Landsberg et al., 2020). Given that tissue necrosis was seen to originate near the coral's algal symbionts (Symbiodiniaceae) in the gastrodermis, it has been hypothesized that SCTLD may be caused by a pathogen or pathogens affecting the symbionts rather than the coral host directly (Work et al., 2021), while the visible lesion and tissue loss may be the result of secondary or opportunistic infection.

The SCTLD pathogen(s) have not yet been identified, though examination of microbiomes of diseased samples suggests a bacterial (Becker et al., 2021; Huntley et al., 2022; Meiling et al., 2021; Meyer et al., 2019; Rosales et al., 2020, 2022, 2023; Studivan et al., 2022; Ushijima et al., 2020) and/or viral (Veglia et al., 2022; Work et al., 2021) consortium. Antibiotic treatments have shown high rates of success in halting the progression of disease lesions, and in some cases, the quiescence of visible disease signs on treated colonies (Forrester et al., 2022; Neely et al., 2020; Shilling et al., 2021; Walker et al., 2021). Attempts to treat SCTLD-affected corals with chlorinated epoxy, which was hypothesized to affect more pathogenic taxa beyond bacteria relative to targeted antibiotics, have been largely unsuccessful (Shilling et al., 2021; Walker et al., 2021). The mechanisms by which antibiotic application affects disease progression are unknown, particularly the potential impacts on the coral host and its microbiome in processes such as recovery and antibiotic resistance.

The molecular mechanisms underlying coral immune responses to SCTLD are poorly understood relative to other diseases (Traylor-Knowles et al., 2022). A recent study utilizing metabolomics identified several lipid and tocopherol classes of Symbiodiniaceae origin that distinguished healthy and diseased corals, providing further evidence of algal symbiont involvement in SCTLD (Deutsch et al., 2021). Transcriptomics have also been used to examine gene expression of disease lesion tissue in multiple coral species, finding a core set of differentially expressed genes across species that are associated with stress, extracellular matrix rearrangement, immunity and apoptosis responses (Beavers et al., 2023; Traylor-Knowles et al., 2021). Several of these pathways are implicated in coral-algal symbiosis and antiviral processes, such as nuclear factor kappa B (NF- κ B) and Ras-related protein rab 7 (rab7), providing further evidence of a potential viral pathogen affecting algal symbionts (Beavers et al., 2023). It is therefore still unknown, however, how antibiotic

treatment is effective if SCTLD is indeed caused by a viral pathogen and how coral immune responses to disease are modulated by antibiotic exposure. To date, no transcriptomic studies of SCTLD, or any coral disease, have focused on the effects of intervention methods, identifying a critical need to understand the potential consequences of antibiotic treatment on coral holobiont responses.

To address this knowledge gap, we conducted paired ex-situ transmission and in-situ intervention experiments and examined whole-transcriptome gene expression patterns of corals in response to disease exposure and antibiotic treatment, respectively. These experiments focused on the coral species *Montastraea cavernosa* and *Orbicella faveolata* due to their ongoing use in field-based disease intervention and monitoring efforts (Shilling et al., 2021; Walker et al., 2021), ecological importance as primary reef-builders (González-Barrios & Álvarez-Filip, 2018; Walton et al., 2018), and growing use in reef restoration (Koval et al., 2020; Rivas et al., 2021). Through these experiments, we (1) identified transcriptomic responses to SCTLD exposure in a controlled lab setting, (2) compared responses to disease exposure between species, (3) examined transcriptomic modulation following antibiotic treatment in a field-based time series and (4) compared trends between diseased and treated corals in lab and field settings. In doing so, we seek to better understand coral immune responses to SCTLD and to provide transcriptomic resources to the development of disease diagnostics. These experiments also evaluated disease intervention effectiveness at the molecular level and identified potential patterns of recovery following antibiotic treatment of SCTLD-affected wild colonies.

2 | METHODS

2.1 | Transmission experiment

The ex-situ transmission experiment was conducted in the Experimental Reef Laboratory at the University of Miami's Cooperative Institute for Marine and Atmospheric Studies over a period of 2 weeks in March 2020. The disease transmission apparatus consisted of 80 0.5-L coral vessels with independent flow-through seawater sources maintained at local ambient temperature (24°C) and light conditions (PAR of 250 $\mu\text{mol m}^{-2}\text{s}^{-1}$; Studivan et al., 2022). Twenty putative genotype fragments each of disease-naïve *O. faveolata* and *M. cavernosa* were sourced from the land-based nursery at Mote Marine Laboratory. Each fragment was split into two equal subfragments for healthy/disease exposure genotype pairs ($N=80$ total) and allowed to recover for 8 days prior to the disease challenge. A disease donor colony of *M. cavernosa* with visible stony coral tissue loss disease (SCTLD) lesions was collected from Broward County, Florida (26.1476, -80.0961) 2 days prior to the start of the experiment, and was cut into ~1×4 cm fragments using a diamond band saw with each fragment containing a portion of active lesion tissue. Coral fragments in the disease-exposed group were maintained in direct contact with diseased tissue fragments, where disease donor fragments were replaced as needed following total loss of tissue.

Genotype pairs in the healthy group were not exposed to any other corals. Corals were observed daily over the course of the experiment to quantify the number of days to onset of disease lesions, as well as to observe the gross signs of lesion formation and tissue necrosis. Following progression of lesions across approximately 50% of the fragment area, coral fragments and their corresponding healthy genotype pair were sampled via a small tissue scrape from near the lesion, which was preserved in TRIzol and flash-frozen in liquid nitrogen. Corals remaining at the end of the experiment were processed in the same manner. Herein, coral fragments are characterized as 'healthy' for all samples in the control group, 'diseased' for samples in the disease-exposed group exhibiting lesions, and 'NAI' (no active infection) for samples in the disease-exposed group that showed no visible signs of disease lesions by the end of the experiment.

2.2 | Intervention experiment

The in-situ intervention experiment was conducted at long-term monitoring site BC1 (mean depth 5.8 m) in Broward County, Florida (26.1476, -80.0961; Combs et al., 2021; Shilling et al., 2021), over 13 days in April–May 2020. Fifteen colonies of *M. cavernosa* with a single visible SCTLD lesion were tagged, and small tissue scrapes were collected ~5 cm from the disease lesion and preserved as described previously. Nineteen visually healthy colonies of the same species were also tagged and sampled. Following the initial sampling, diseased colonies were treated with amoxicillin in CoreRx Base 2B as described in Shilling et al. (2021), with the exception that trenching of the coral skeleton in advance of the disease lesion was not conducted. Colonies were then revisited 13 days later, and tissue sampling was repeated. No new lesions were reported on any colonies over the duration of the sampling period.

2.3 | Tag-Seq library preparation, sequencing, and bioinformatics

Total RNA was extracted in samples from both experiments using modified versions of protocols for the Zymo Direct-zol RNA Mini-prep and Zymo RNA Clean & Concentrator-5 kits (Studivan, 2022c). RNA was quantified on an Agilent Bioanalyzer 2100 and analyzed for purity on a Nanodrop 1000, where samples with RIN scores <4 or poor purity ratios were re-extracted. All successfully extracted samples were normalized to 60 ng/μL and sent to the University of Texas at Austin Genome Sequencing and Analysis Facility for library preparation and sequencing. Tag-Seq library preparation was performed in duplicate using 600 ng of initial RNA for *M. cavernosa* samples and 100 ng for *O. faveolata* samples due to initial issues with PCR inhibitors in the latter. Following successful amplification of all samples, libraries were pooled and sequenced on a NovaSeq 6000 S2-XP flow cell generating 1×100 bp reads with 20% PhiX spike-in for a target read depth of ~10 million reads per library (~20 million reads per sample).

Raw sequences were processed according to custom Perl scripts in a GitHub repository release (Studivan, 2022c) to deduplicate, trim (FASTX-Toolkit; Gordon & Hannon, 2010), align (Bowtie 2; Langmead & Salzberg, 2012) and quantify gene counts (SAMtools; Danecek et al., 2021) for each sample. Dominant symbiont genera were determined by aligning sample reads to a reference containing Symbiodinaceae 28S sequences across the four main genera (*Symbiodinium* spp., *Breviolum* spp., *Cladocopium* spp. and *Durusdinum* spp.). *Montastraea cavernosa* samples were dominated by *Cladocopium* spp. (99.7%), and *O. faveolata* samples contained a majority of *Durusdinum* spp. alignments (93.4%). Cleaned reads were mapped to separate host (*M. cavernosa*, Kitchen et al., 2015; *O. faveolata*, Pinzón et al., 2015) and algal symbiont (*Cladocopium* spp., Davies et al., 2018; *Durusdinum* spp., Shoguchi et al., 2021, respectively) reference transcriptomes sequentially to remove cross-contaminated sequences in both host and symbiont transcriptomes. Transcriptome annotations for host and symbiont references were created according to GitHub repositories for *O. faveolata* (Studivan, 2022b) and *M. cavernosa* (Studivan, 2022a) using eggNOG-Mapper (Huerta-Cepas et al., 2016, 2018).

Following deduplication, the mean number of reads across all samples was 24.6 ± 0.9 million, with 5.8 ± 0.2 million reads remaining following trimming and cleaning. For *M. cavernosa* samples, alignment was $61.2 \pm 0.7\%$ for host and $6.5 \pm 0.3\%$ for symbionts with 82,594 and 32,862 isogroups, respectively. The original version of the *M. cavernosa* transcriptome was chosen over the updated, genome-derived version (<https://matzlab.weebly.com/data--code.html>) due to low alignment in the latter ($28.0 \pm 0.3\%$ for host and $7.1 \pm 0.4\%$ for symbiont) and poorer representation of isogroups (24,850 and 32,932 isogroups, respectively) for downstream differential expression analysis. Alignment rates for *O. faveolata* samples were $60.3 \pm 1.6\%$ for host and $15.6 \pm 0.8\%$ for symbionts, resulting in 81,960 and 39,854 isogroups, respectively.

2.4 | Statistical analysis

All statistical analyses were conducted in the R statistical environment (R Core Team, 2021). Analysis scripts and outputs can be found in a GitHub repository release associated with this manuscript (Studivan, 2023). Transmission metrics from the transmission experiment (time to onset of disease lesions) were analysed for an effect of species using an ANOVA of Box-Cox transformed data and with a fit proportional hazards regression model in the packages *survival* (Therneau, 2021) and *survminer* (Kassambara et al., 2021) to determine the relative risk of developing disease lesions between species.

For transcriptomic data, aligned gene counts were first separated by experiment, species, and host/symbiont datasets and then pre-filtered to remove isogroups with a cumulative count <10 across all samples. Data were subsequently transformed using a variance stabilizing transformation in the *DESeq2* package (Love et al., 2014) and examined for outlier samples using the package *arrayQualityMetrics* (Kauffmann et al., 2009). Samples violating the distance between sample arrays criterion (S_a) were removed from the respective

experiment and host/symbiont datasets (Tables 1 and 2). Significance testing for the transmission experiment datasets was performed with PERMANOVA using $1e^6$ permutations, and sample dispersion was visualized using PCoA of Manhattan distance in the package *vegan* (Oksanen et al., 2015). Discriminant analysis of principal components (DAPC) in the *adegenet* package (Jombart, 2008) was used for the intervention experiment datasets to test the magnitude of transcriptomic plasticity in amoxicillin-treated corals relative to diseased and healthy controls, with significance testing in the package *MCMCglmm* (Hadfield, 2010). Differential expression analyses were conducted using *DESeq2* models for the respective experiments. For *M. cavernosa* in the transmission experiment, the model genotype + disease status ('healthy', 'diseased', and 'naï') was used since not all fragments exhibited disease signs, whereas for *O. faveolata*, the model genotype + exposure group ('control' and 'sctld') was used. For the intervention experiment, a single-factor concatenated treatment and time ('control.0', 'sctld.0', 'control.1' and 'sctld.1') model was used. Contrast statements were used to conduct pairwise comparisons for each of the experiment datasets as described in the GitHub repository release (Studivan, 2023). Visualization of differentially expressed genes (DEGs) was done using the *pheatmap* package (Kolde, 2019).

Functional enrichment analyses with Mann–Whitney U tests were conducted for each experiment's pairwise comparisons using the packages KOGMWU (Dixon et al., 2015) of log fold change data (lfc) and GO-MWU (Wright et al., 2015) of log *p* value data (lpv) with an alpha cut-off of .05 for eukaryotic orthologous group (KOG) and gene ontology (GO) annotations, respectively. To identify correlational relationships between gene modules (genes with similar expression patterns) and experimental variables, weighted gene co-expression network analyses (WGCNA; Langfelder & Horvath, 2008) were conducted as described in the associated GitHub repository release (Studivan, 2023). Module-associated genes were then exported for GO enrichment analysis to examine any relationships between gene expression patterns and additional sample traits beyond diseased versus healthy status. Module hub genes (i.e., genes with the maximum adjacency to other genes in the module, which may infer biological function) were run through the InterPro database to classify protein families and/or domains (Paysan-Lafosse et al., 2023).

Finally, DEGs unique to and shared between species and experiments were determined using the *VennDiagram* package (Chen &

Boutros, 2011). For the transmission experiment, common DEGs (orthogroups) and associated KOG/GO annotations for diseased/healthy comparisons in *M. cavernosa* and *O. faveolata* were identified by blast annotations using OrthoFinder (Emms & Kelly, 2015, 2019) and visualized by heatmaps and KOG classes. For comparison of DEGs in *M. cavernosa* samples from the transmission and intervention experiments (e.g., to compare DEGs in disease-exposed transmission samples to antibiotic-treated samples in the intervention experiment), matching gene and KOG annotations were examined in the same fashion as the cross-species comparisons. DEGs with known immune function related to SCTLD exposure (Beavers et al., 2023; Traylor-Knowles et al., 2021) were identified in the datasets and tested for significant differences among treatment groups with one-way ANOVAs and Tukey's post hoc tests then visualized using boxplots.

3 | RESULTS

3.1 | Transmission experiment

3.1.1 | Transmission metrics

There was a significant difference in the number of days to the onset of visible disease lesions between species (ANOVA: $F_{1,29}=6.22$, $p<.019$), with *O. faveolata* significantly more likely to develop stony coral tissue loss disease (SCTLD) lesions compared to *M. cavernosa* (log-rank: $z_{1,29}=3.569$, $p<.001$; Figure S1). Transmission rates in the disease-exposed treatment at the conclusion of the experiment

TABLE 2 Sample sizes for the intervention experiment, where n_{treat} denotes treatment sample sizes and n_{host} and n_{sym} denote the number of samples used for host and symbiont differential gene expression analyses, respectively.

Time point	Treatment	n_{treat}	n_{host}	n_{sym}
2020-04-21 (t_0)	Healthy	19	15	15
	Diseased	15	15	15
2020-05-04 (t_1)	Healthy	19	15	14
	Treated	15	15	13

TABLE 1 Sample sizes and transmission metrics for the transmission experiment including proportion of individuals exhibiting disease lesions (transmission rate) and the time to onset of lesions (mean days to transmission).

Species	Treatment	n_{treat}	n_{host}	n_{sym}	n_{lesion}	Transmission rate	Days to transmission (mean \pm SEM)
<i>Montastraea cavernosa</i>	Control	20	20	18	0	0%	N/A
	SCTLD	20	19	18	11	55%	5.4 \pm 1.0
<i>Orbicella faveolata</i>	Control	20	19	20	0	0%	N/A
	SCTLD	20	18	14	19	95%	3.1 \pm 0.5

Note: Treatment sample size denoted by n_{treat} and the number of samples exhibiting lesions as n_{lesion} , with samples used for host and symbiont differential gene expression analyses as n_{host} and n_{sym} , respectively.

were 95% for *O. faveolata* with lesions occurring at a mean of 3.1 ± 0.5 days, while 55% of *M. cavernosa* fragments exhibited lesions at a mean of 5.4 ± 1.0 days (Table 1). No controls in either species developed lesions. Visible signs of SCTLD were similar between species, with tissue necrosis and lesion formation/progression being the most common (Dataset S1).

3.1.2 | Differential expression

Analysis of Tag-Seq data with two-way PERMANOVAs identified significant effects of coral genotype and disease status on gene expression of *M. cavernosa* and *Cladocopium* symbionts. Ordination with PCoAs for *M. cavernosa* demonstrated that diseased samples

were distinct from all other samples, while no active infection (NAI) and healthy samples were more similar (Figure 1). This relationship was reversed for *Cladocopium* data, where diseased and NAI samples were more closely related to each other than to healthy samples. Pairwise differential expression tests with DESeq2 indicated the majority of differentially expressed genes (DEGs) to be attributed to diseased versus healthy samples for *M. cavernosa* (3890 upregulated and 3878 downregulated), with 1820 DEGs between diseased and samples not exhibiting visible disease signs following exposure (NAI; 960 upregulated and 860 downregulated), and 115 DEGs between NAI and healthy samples (43 upregulated, 72 downregulated). Few DEGs were identified for any pairwise comparisons in *Cladocopium* symbionts, with five in diseased versus healthy samples and two in NAI versus healthy samples.

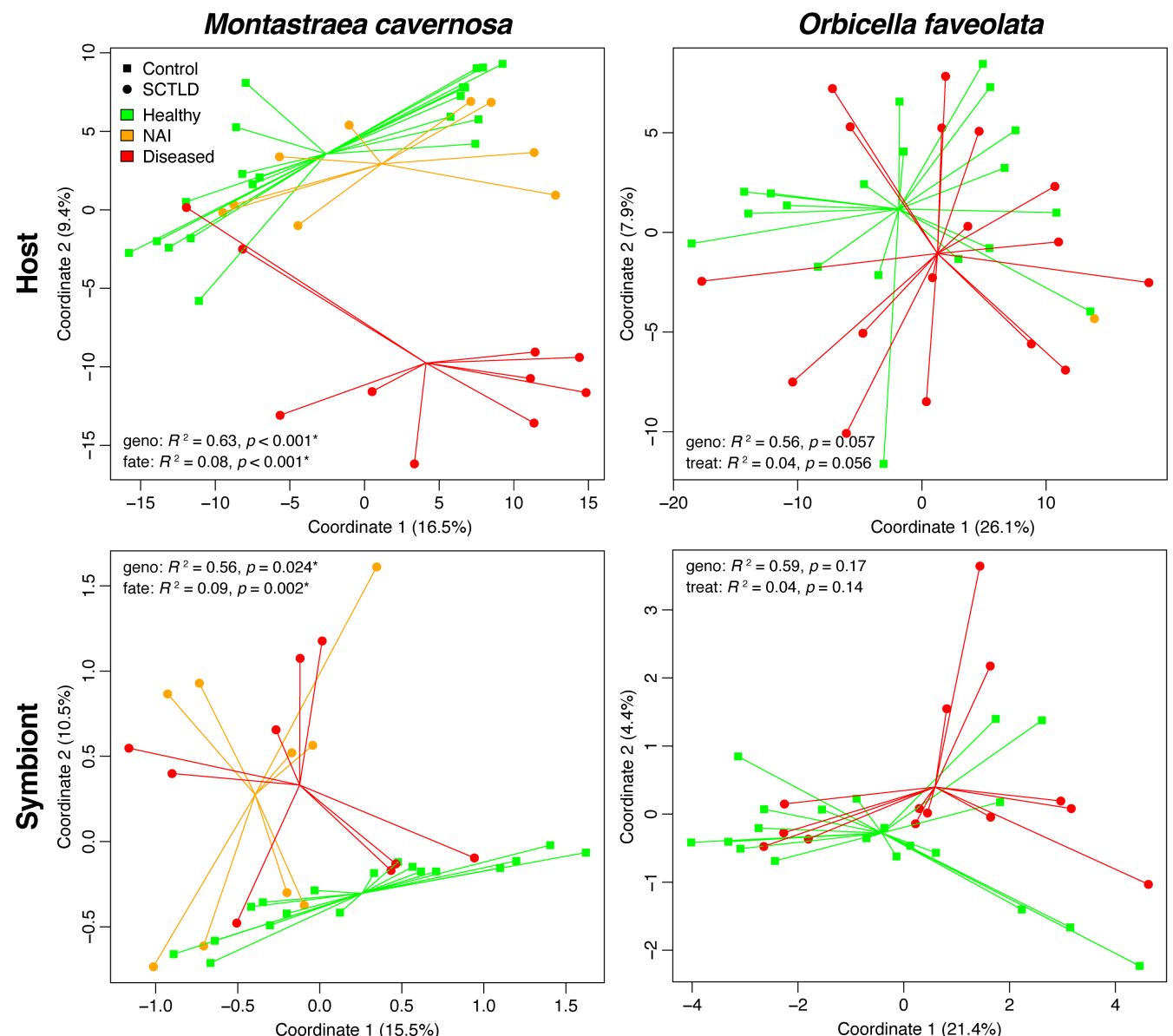


FIGURE 1 PCoAs of coral species and associated symbionts from the transmission experiment, visualizing sample variation among treatments (control and SCTLD-exposed; shapes) and disease status (healthy, no active infection [NAI] and diseased; colours). Test statistics from PERMANOVA models and axis percentages indicate the amount of variation explained by the respective coordinate.

PERMANOVA effects of genotype and exposure group were marginally insignificant for *O. faveolata* ($p=.057$ and $p=.056$, respectively) and non-significant for associated *Durusdinium* symbionts (Table 3). Both *O. faveolata* and *Durusdinium* samples showed similarities between healthy and diseased samples, with high overlap between exposure groups in the ordination space (Figure 1). *Orbicella faveolata* showed moderate numbers of DEGs between diseased and healthy samples (385 upregulated and 188 downregulated) with no DEGs for *Durusdinium* (Table 4).

3.1.3 | Functional enrichment

Functional enrichment analysis of eukaryotic orthologous groups (KOGs) demonstrated similar patterns between diseased versus healthy and diseased versus NAI samples for *M. cavernosa* (Figure S2), where metabolic and transport mechanisms were generally downregulated in diseased samples, and nuclear structure and translation-related pathways were upregulated. Some nuclear structure and membrane pathways were positively enriched in NAI versus healthy *M. cavernosa*, with downregulation of translation, cytoskeleton and extracellular pathways. *Cladocopium* diseased and NAI samples showed enrichment of most pathways relative to healthy controls, with nuclear structure as the most positively enriched and cell motility as the most downregulated. Similar trends were observed for diseased versus healthy *O. faveolata* as compared to *M. cavernosa*, including downregulation of metabolic and transport pathways and upregulation of nuclear and translation mechanisms. *Durusdinium* showed an inverse pattern of KOG enrichment in diseased samples relative to *Cladocopium* through weak

upregulation of repair mechanisms, strong suppression of nuclear and extracellular structures, and strong upregulation of cell motility (Figure S2).

Functional enrichment using gene ontology (GO) identified 434 GO terms across three categories (molecular function [MF]: 38; biological process [BP]: 287; cellular component [CC]: 109) for diseased versus healthy *M. cavernosa* samples (Table S1). Of these, the most significantly enriched GO terms with upregulated genes in diseased samples were RNA binding (MF, GO:0003723), intracellular protein transport (BP, GO:0006886), response to endoplasmic reticulum stress (BP, GO:0034976), cilium movement (BP, GO:0003341) and plasma membrane bounded cell projection cytoplasm (CC, GO:0032838, GO:0005930, GO:0097014), while the most significant downregulated terms in diseased samples were catalytic activity acting on DNA (MF, GO:0140097), DNA replication and DNA-dependent DNA replication (BP, GO:0006261 and GO:0006260) and lysosomal lumen (CC, GO:0043202). For diseased versus NAI *M. cavernosa*, 371 GO terms were significantly enriched (MF: 50; BP: 244; CC: 77), where the most significantly enriched GO terms in diseased versus healthy individuals described above were represented here. Only eight terms were significantly enriched for NAI versus healthy samples (BP: 2; CC: 6; Table S2), with the only significant upregulated term being cilium movement (BP, GO:0003341), and the most significant downregulated terms in NAI versus healthy being cytokinesis (BP, GO:0061640, GO:0000910), endoplasmic reticulum lumen (CC, GO:0005788) and extracellular region part (CC, GO:0005615, GO:0044421). The majority of enriched GO terms were downregulated in diseased versus healthy and diseased versus NAI *M. cavernosa*, indicating a general suppression of transcriptomic activity following disease lesion formation.

TABLE 3 Test statistics for differential gene expression analyses by experiment, test type, host species, and associated symbionts across treatment factors.

Experiment	Test	Species	Factor	df	Test statistic	R ²	p
Transmission	PERMANOVA	<i>Montastraea cavernosa</i>	Genotype	19	1.955	.6282	<.001
			Status	2	2.489	.0842	<.001
		<i>Cladocopium</i> spp.	Genotype	19	1.1746	.5607	.024
	DAPC	<i>Orbicella faveolata</i>	Status	2	1.7443	.0876	.002
			Genotype	19	1.2049	.5641	.057
		<i>Durusdinium</i> spp.	Treatment	1	1.6927	.0417	.056
Intervention	DAPC	<i>Montastraea cavernosa</i>	Genotype	19	1.1	.5945	ns
			Treatment	1	1.2558	.0357	ns
		<i>Cladocopium</i> spp.	treated1_diseased0				<.001
			healthy0_diseased0				<.001
	MCMC	<i>Cladocopium</i> spp.	healthy1_diseased0				<.001
			treated1_healthy1				ns
		<i>Cladocopium</i> spp.	treated1_diseased0				<.001
			healthy0_diseased0				.024
	DAPC	<i>Cladocopium</i> spp.	healthy1_diseased0				<.001
			treated1_healthy1				<.001

Note: Non-significant p values denoted as ns.

TABLE 4 Differentially expressed genes (DEGs) by experiment, host species, and associated symbionts across treatment pairwise comparisons.

Experiment	Species	Comparison	Host DEGs			Sym DEGs		
			Up	Down	Total	Up	Down	Total
Transmission	<i>Montastraea cavernosa</i>	diseased_healthy	3890	3878	7768	4	1	5
		nai_healthy	43	72	115	2	0	2
		diseased_nai	960	860	1820	0	0	0
	<i>Orbicella faveolata</i>	diseased_healthy	385	188	573	0	0	0
Intervention	<i>Montastraea cavernosa</i>	diseased0_healthy0	284	126	410	0	0	0
		treated1_diseased0	48	193	241	0	0	0
		treated1_healthy1	4	1	5	0	0	0
		healthy1_healthy0	183	65	248	8	4	12
		treated1_healthy0	269	246	515	5	7	12
		diseased0_healthy1	128	137	265	1	1	2

Note: Up denotes DEGs with higher relative expression in treatment x/treatment y, and down denotes lower relative expression.

In *O. faveolata*, 45 GO terms were enriched in diseased versus healthy samples (MF: 9; BP: 20; CC: 16; **Table S1**), and the majority of enriched terms were upregulated in diseased versus healthy samples for this species. The most significantly enriched GO terms upregulated in diseased individuals relative to healthy controls were structural constituent of ribosome (MF, GO:0003735), cytoplasmic translation (BP, GO:0002181), cytosolic ribosome and cytosolic large ribosomal subunit (CC, GO:0022626 and GO:0022625); the most significantly downregulated GO terms were active transmembrane transporter activity (MF, GO:0022804), cofactor transport (BP, GO:0051181) and intrinsic component of plasma membrane (CC, GO:0005887, GO:0031226). No GO terms were significantly enriched for *Cladocopium* or *Durusdinum* symbionts.

3.1.4 | Weighted gene coexpression network analysis

Weighted gene coexpression network analysis (WGCNA) identified 10 modules with significant correlations to experimental factors (disease status and the time to onset of lesions) in *M. cavernosa*. In general, modules that were negatively correlated with healthy samples were positively correlated with diseased samples (**Figure S3**). Several modules were also correlated with NAI samples that demonstrated similar expression to diseased samples (module 'darkorange2') and the time to transmission ('thistle1' and 'darkorange2'), or inverse relationships with healthy samples ('navajowhite1'). Five module hub genes (i.e., genes with the highest number connections to other genes in the module) had protein domain annotations for *M. cavernosa*, all of which modules had significant correlations to experimental traits. Their function included known immunity protein domains/families such as growth factor receptor ('blue2') and proteasome B-type subunit ('darkorange2'). The hub gene for module 'darkseagreen4', tropomyosin, was downregulated in response to SCTLD exposure in our study and in a recent experiment by Beavers

et al. (2023; **Table S3**). The hub gene for module 'royalblue', insulin-like growth factor-binding protein, was associated with a significant positive correlation with NAI samples. Of the modules correlated with NAI samples, only 'darkorange2' showed significant GO enrichment to the mRNA metabolic process (BP) and peptidase, cytosolic, and ribosomal complexes (CC; **Table S4**). Four modules were found to have significant trait correlations for *Cladocopium*, with similar expression patterns between NAI and diseased samples relative to healthy controls in the 'pink' module, but no significant GO enrichment. Four modules had protein domain-annotated hub genes, only one of which had a significant negative correlation with the transmission time (translation initiation factor IF-2, module 'red'; **Table S3**).

The *O. faveolata* dataset had six modules with significant correlations to disease status and the time to onset of lesions; most of these were inversely related between diseased and healthy samples, apart from the 'tan' module that was inversely related between NAI and healthy samples (**Figure S3**). There were no significantly enriched GO terms for the 'pink' or 'tan' modules correlated with NAI samples. Six module hub genes had protein domain annotations for *O. faveolata*, two of which had significant correlations with experimental traits: ATP synthase (module 'black') that was negatively correlated with transmission time, and calcium ion binding ('greenyellow') that was negatively correlated with disease (**Figure S3**). An immune-related hub gene was identified for module 'purple', mannose-6-phosphate receptor, but the module did not have any significant correlations. WGCNA was not successful in assigning modules to the *Durusdinum* dataset.

3.1.5 | Orthologous genes

Orthofinder identified 681 orthologous DEGs in diseased versus healthy samples between species; of these, 438 showed similar expression patterns (272 upregulated and 166 downregulated), and 243 showed inverse expression (**Figure 2**). Only two orthologous

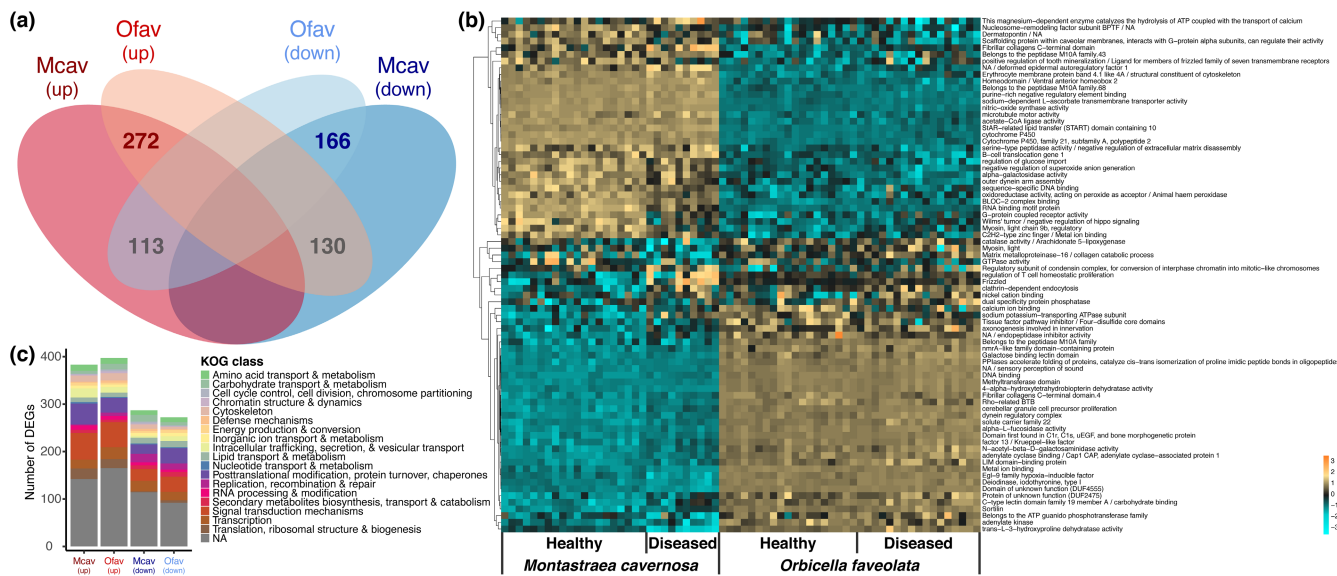


FIGURE 2 (a) Common genes (orthogroups) in diseased versus healthy corals compared between *Montastraea cavernosa* (Mcav) and *Orbicella faveolata* (Ofav) samples from the transmission experiment, denoting higher relative expression in diseased/healthy as red (up) and lower expression as blue (down). (b) Heatmap of most significant genes (cut-off 10^{-6}) across disease state and species. (c) Representation of eukaryotic orthologous groups (KOGs) across common genes for relative expression levels (up, down) and species.

DEGs identified as part of the immune response to SCTLD were identified in both species (spondin2b and animal haem peroxidase); spondin2b was shown to have decreased expression in diseased versus healthy samples (though not significant for *M. cavernosa*), and animal haem peroxidase showed a significant difference in diseased and healthy samples with an inverse relationship between species (Figure S4). There were 19 additional genes known to be associated with previously reported immune processes with significant variation in expression levels across fates in *M. cavernosa* (Figure S5), and 12 significant genes in *O. faveolata* (Figure S6). These included two apoptosis regulation pathways that were differentially expressed in diseased *M. cavernosa* relative to healthy controls. Extracellular matrix genes (four for *M. cavernosa* and two for *O. faveolata*, both including spondin2b mentioned above) were downregulated in SCTLD-affected corals for both species, except for one gene in *M. cavernosa* that was also associated with the transforming growth factor-beta (TGF- β) immune pathway. Three TGF- β genes were downregulated in diseased versus healthy *M. cavernosa*. One NF- κ B activation gene was upregulated in diseased versus healthy *M. cavernosa*, while two were found to be higher expressed in diseased *O. faveolata* relative to healthy controls. Three peroxidases were upregulated in diseased *M. cavernosa*, but of the seven differentially expressed peroxidase genes in *O. faveolata*, four were downregulated in diseased versus healthy controls. Protein tyrosine kinase genes (PTK; seven in *M. cavernosa* and one in *O. faveolata*) were mostly upregulated in diseased versus healthy individuals, although two genes showed downregulation in diseased *M. cavernosa* (Figure S5). Finally, one WD repeat gene was downregulated in diseased *O. faveolata* relative to healthy controls (Figure S6).

While the expression of individual genes was in some cases inversely related between species (Figure 2), the corresponding KOG

annotations demonstrated that the number of DEGs within each KOG class that was up- or downregulated was relatively similar, suggestive of an overall similar functional response to disease exposure between *M. cavernosa* and *O. faveolata*. Likewise, the examination of GO categories in diseased versus healthy samples indicated 21 GO terms (MF: 2; BP: 11; CC: 8) that were commonly enriched in the same direction between species (Table 5; Figure 3). GO terms encompassing protein translation, transport, and metabolism were upregulated in diseased samples between species, while meiosis and DNA metabolic processes were suppressed in diseased individuals.

3.2 | Intervention experiment

3.2.1 | Differential expression

Discriminant analysis of principal components (DAPCs) indicated that expression in the diseased corals and their associated symbionts was significantly different from all other treatment groups including the post-treatment samples (Table 3). MCMC significance testing revealed that treated corals were indistinguishable from healthy controls at t_1 for host gene expression ($p=.98$), but not for algal expression ($p<.001$). In both datasets, however, gene expression of treated colonies more resembled that of the healthy controls compared to the original diseased state (Figure 4); indeed, DAPC assigned 80% of treated corals to the healthy t_1 group in the coral dataset and 23% in the algal dataset (the remaining 77% were assigned to the healthy t_0 group; Table S5). Differential expression analyses identified DEGs associated with pairwise treatment/time comparisons, with the most number of DEGs between diseased and healthy corals at t_0 (410 DEGs: 284 upregulated and

TABLE 5 Matching enriched gene ontology (GO) terms across species for the transmission experiment, separated by GO categories: molecular function (MF), biological process (BP), and cellular component (CC).

		<i>Montastraea cavernosa</i>				<i>Orbicella faveolata</i>			
GO category	GO name	GO terms	p Value	Direction	Genes	GO terms	p Value	Direction	Genes
MF	RNA-binding	GO:0003723	9.25E-05	Up	139	GO:0003723	.033	Up	64
MF	Structural constituent of ribosome	GO:0003735	.001	Up	45	GO:0003735	1.47E-14	Up	20
BP	Cytoplasmic translation	GO:0002181	3.51E-09	Up	44	GO:0002181	1.05E-15	Up	19
BP	DNA metabolic process	GO:0006259	1.41E-09	Down	130	GO:0006259	.035	Down	51
BP	Establishment of protein localization to membrane	GO:0090150	1.82E-07	Up	52	GO:0090150	.002	Up	18
BP	Intracellular protein transport	GO:0006886	1.01E-15	Up	170	GO:0006886	.001	Up	70
BP	Mitosis I cell cycle process	GO:0061982; GO:0007127	4.24E-05	Down	30	GO:0061982	.031	Down	17
BP	Nuclear-transcribed mRNA catabolic process, nonsense-mediated decay	GO:0000184	4.01E-05	Up	28	GO:0000184	.001	Up	11
BP	Peptide biosynthetic process	GO:0006412; GO:0043043	5.60E-07	Up	95	GO:0006412; GO:0043043	3.11E-06	Up	37
BP	Peptide metabolic process	GO:0043604; GO:0006518	.001	Up	145	GO:0013604; GO:0006518	.001	Up	60
BP	Protein targeting	GO:0006605	3.94E-07	Up	75	GO:0006605	.019	Up	23
BP	Protein targeting to membrane	GO:0006612; GO:0045047; GO:0072599; GO:0070972	1.59E-08	Up	48	GO:0006612	7.02E-05	Up	11
BP	Translational initiation	GO:0006413	1.60E-08	Up	42	GO:0006413	.001	Up	16
CC	Cytosolic large ribosomal subunit	GO:0022625	3.65E-06	Up	30	GO:0022625	8.00E-13	Up	13
CC	Cytosolic part	GO:0044445	6.45E-06	Up	63	GO:0044445	9.78E-07	Up	30
CC	Cytosolic ribosome	GO:0022626	1.60E-07	Up	46	GO:0022626	2.71E-15	Up	20
CC	Cytosolic small ribosomal subunit	GO:0022627	.010	Up	15	GO:0022627	8.96E-06	Up	6
CC	Large ribosomal subunit	GO:0015934	.001	Up	32	GO:0015934	1.25E-08	Up	15
CC	Polysome	GO:0005844	.001	Up	21	GO:0005844	.035	Up	13
CC	Ribonucleoprotein complex	GO:1990904	2.75E-06	Up	145	GO:1990904	.009	Up	69
CC	Ribosome	GO:0005840; GO:0044391	.0002	Up	54	GO:0005840; GO:0044391	1.91E-10	Up	26

Note: FDR-corrected p values correspond to results of Mann–Whitney *U* tests on pairwise contrasts of diseased/healthy samples for each species.

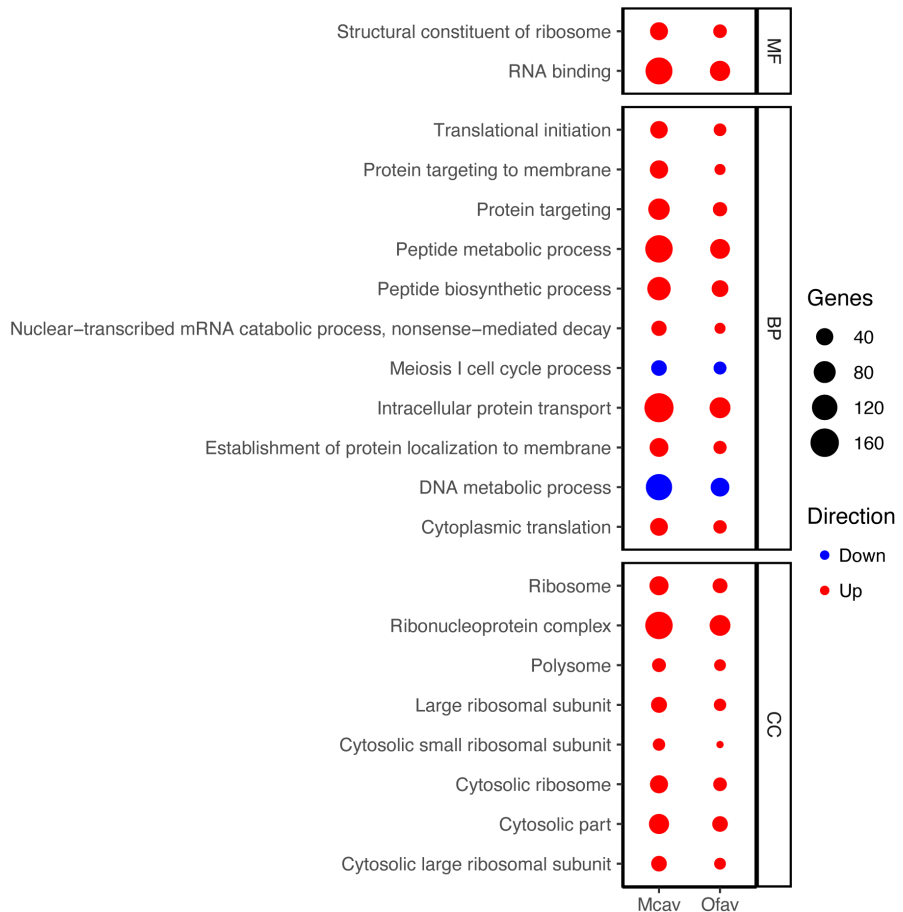


FIGURE 3 Bubble plot of matching enriched gene ontology (GO) terms across species (Mcav: *Montastraea cavernosa*; Ofav: *Orbicella faveolata*) for the transmission experiment. The size of the bubble corresponds to the number of genes enriched within the GO term, the color denotes the direction of enrichment, and panels separate GO categories molecular function (MF), biological process (BP), and cellular component (CC).

126 downregulated), the second being between amoxicillin-treated corals at t_1 and their original diseased state at t_0 (241 DEGs: 48 upregulated and 193 downregulated; Table 4; Figure 4). There were few differences between treated and healthy corals at t_1 (5 DEGs: 4 upregulated and 1 downregulated), and temporal shifts in gene expression were evident (e.g., 248 DEGs in t_1 vs. t_0 healthy corals). Few DEGs were identified across pairwise comparisons for *Cladocopium* (Table 4; Figure 4).

Identification of immune-related pathways with significant variation across treatments revealed five genes: two PTK genes, one of which was elevated in diseased colonies but not in their post-treatment state or in healthy controls, and another that showed significant upregulation in treated versus diseased and healthy corals (Figure S7). Three WD repeat genes were also found, one of which showed upregulation in treated corals relative to diseased and healthy controls, while the remaining two had significantly higher expression in diseased individuals versus both other treatments (Figure S7).

3.2.2 | Functional enrichment

KOG enrichment in diseased versus healthy corals at t_0 was similar to the trends observed for the transmission experiment, where several metabolic and transport pathways were negatively enriched (Figure 5). Notably, the nuclear structure KOG class was highly

downregulated in diseased corals, when it was shown to be upregulated for both diseased *M. cavernosa* and *O. faveolata* samples from the transmission experiment. Comparison of treated versus diseased corals demonstrated an opposite response in the same pathways as compared to diseased versus healthy corals, showing an increase in metabolic, transport and nuclear structure classes. No KOG classes were strongly enriched when comparing treated and healthy corals at t_1 . *Cladocopium* KOG enrichment was similar in diseased versus healthy corals to the transmission experiment samples, with strong upregulation of nuclear structure and suppression of cell motility. Following treatment with amoxicillin, those patterns were reversed, even when comparing treated to healthy corals at t_1 (Figure 5).

GO enrichment analysis identified 46 significantly enriched GO terms in diseased versus healthy corals at t_0 (MF: 9; BP: 10; CC: 27; Table S6; Figure S8). Similar to diseased *M. cavernosa* samples from the transmission experiment, the majority of enriched GO terms were negatively enriched in diseased versus healthy corals in the intervention experiment, broadly including downregulated protein synthesis and transport, endoplasmic reticulum processes, and oxidoreductase activity. Conversely, relatively few GO terms were upregulated: microtubule processes and ubiquitin, the latter of which is part of NF-κB pathway activation (Beavers et al., 2023). There were 39 significant GO terms in treated versus diseased corals (MF: 6; BP: 14; CC: 19), with the majority upregulated in treated corals including those described above that were suppressed in diseased corals:

protein translation, metabolism, and transport, as well as endoplasmic reticulum processes and oxidoreductase activity. Microtubule processes and ciliary structures were downregulated following treatment (Figure S8). Seven GO terms were significantly enriched in treated versus healthy corals at t_1 (MF: 1; CC: 6): endoplasmic reticulum terms were upregulated in treated versus healthy samples at t_1 , and ciliary structures and plasma membrane components were downregulated (Table S6; Figure S8).

3.2.3 | Weighted gene coexpression network analysis

WGCNA returned eight modules significantly correlated with treatments/time points, with the strongest patterns of inverse correlations

between healthy corals at t_0 to t_1 (modules 'darkred' and 'salmon'; Figure 6). Modules 'greenyellow' and 'purple' showed inverse correlations between diseased and healthy corals at t_0 , and only the 'pink' module showed an inverse relationship between treated and diseased corals. Only the 'darkred' module contained significantly enriched GO terms, all of which were downregulated endoplasmic reticulum complexes (CC; Table S4). Visualization of expression patterns for the 30 most significant DEGs in modules 'greenyellow' and 'grey60' demonstrated a shift in expression patterns from the original disease state being distinct to healthy controls, to overall similarities between treated and healthy corals (Figure 6). Nine module hub genes had corresponding protein domain annotations, four of which were associated with significant experiment trait correlations: the heat shock protein 70 family (module 'darkred') was downregulated over time in the healthy controls, fibrillar collagen ('grey60') was downregulated

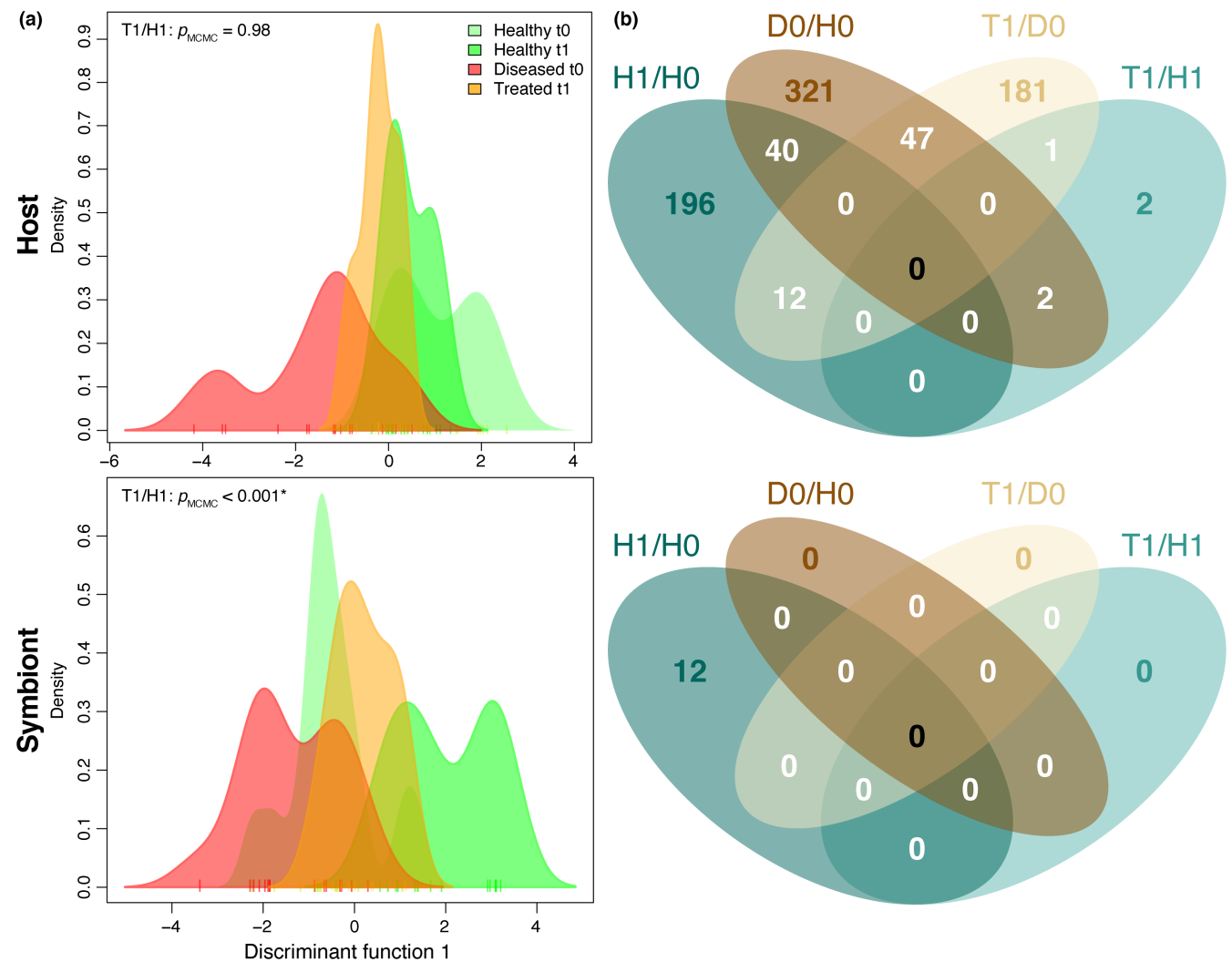


FIGURE 4 (a) Discriminant analysis of principal components (DAPCs) of *Montastraea cavernosa* samples and associated symbionts from the intervention experiment, visualizing sample assignments among a single-factor combination of treatments and sampling time points. Test statistics from MCMC generalized linear models denote similarities of the treated treatment to the original disease state and the healthy controls at t_1 , where a significant result indicates that treated corals were more similar to one treatment group over another. (b) Venn diagrams of common DEGs across pairwise comparisons of treatments/time (H1/H0: Healthy t_1 /Healthy t_0 ; D0/H0: Diseased t_0 /Healthy t_0 ; T1/D0: Treated t_1 /Diseased t_0 ; T1/H1: Treated t_1 /Healthy t_1).

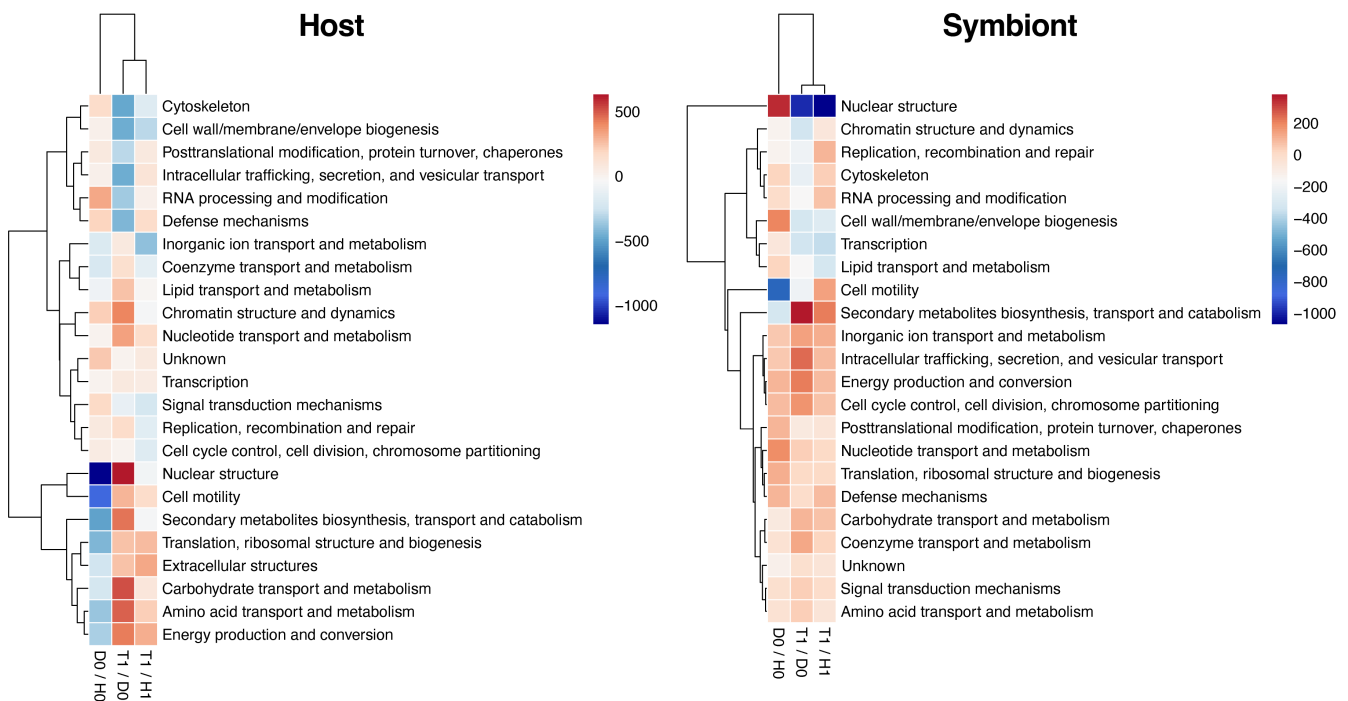


FIGURE 5 Heatmaps of eukaryotic orthologous group (KOG; rows) enrichment between pairwise comparisons of treatments (columns) for the intervention experiment, separated by coral host and associated symbionts. Color values represent Mann-Whitney *U* test ranks for each dataset, and hierarchical networks denote similarities among KOG classes and treatment pairwise comparisons, respectively. KOG enrichment calculated using DEGs (\log_2 fold change).

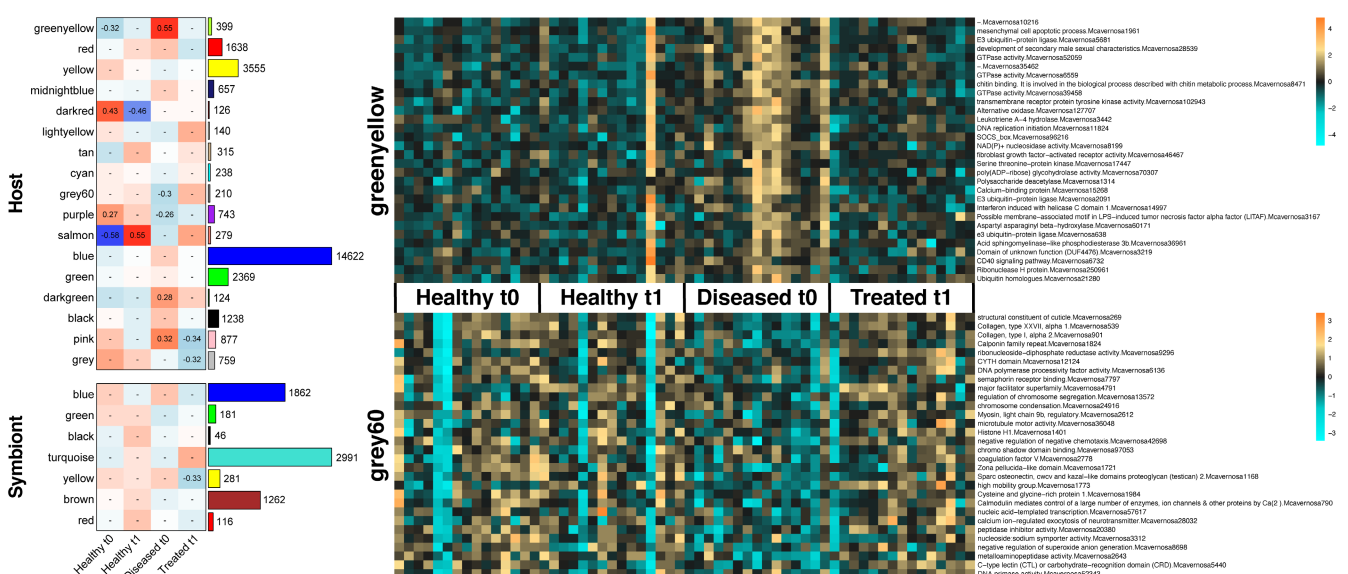


FIGURE 6 Correlational heatmaps of weighted gene coexpression network analysis (WGCNA) modules across treatments for the intervention experiment, separated by coral host and associated algal symbionts. Cell colors correspond to the direction of the correlation (red: positive; blue: negative), numbers correspond to significant correlation coefficients, and barplots denote the number of genes within each module. Heatmaps represent expression patterns of the top 30 most significantly differentially expressed genes within the 'greenyellow' and 'grey60' modules.

in diseased corals, heat shock transcription factor ('pink') was upregulated in diseased corals and downregulated in treated corals, and NAD-dependent epimerase/dehydratase ('salmon') was strongly upregulated in healthy controls over time (**Figure 6**). One module had

a significant correlation to experimental traits in *Cladocopium*, but it was driven by one sample and therefore disregarded. Of note was the hub gene of module 'turquoise', photosystem II PsbL, though it was not significantly correlated with any experiment traits.

3.3 | Cross-experiment comparisons

Comparison of diseased versus healthy *M. cavernosa* samples from the transmission and intervention experiments revealed 1458 genes that were significantly differentially expressed in both experiments. The majority of common genes in diseased samples showed the same directionality between experiments (452 upregulated and 489 downregulated), while 517 genes showed inverse relationships between experiments (*Figure S9*). When comparing diseased versus healthy samples in the transmission experiment to treated versus diseased corals in the intervention experiment, however, the majority of genes were found in inverse relationships between experiments (1041 genes), whereas only 285 genes were found to share the same direction of expression (121 upregulated and 164 downregulated). Three immune-related genes were identified across both experiments as having significant variation in expression among the respective treatments. Diseased individuals were found to have the highest upregulation of a peroxidase gene relative to healthy controls and treated individuals, with no significant differences between healthy controls and treated corals in the intervention experiment, nor differences between healthy controls and NAI corals in the transmission experiment (*Figure S10*). Two TGF- β genes showed relative suppression in diseased versus treated and NAI corals, respectively. Gene representation within KOG classes was largely similar across experiments, with the exception of unannotated genes that contributed to variability between experiments and among disease status/treatment comparisons (*Figure S9*).

4 | DISCUSSION

4.1 | Strong transcriptional responses to SCTLD challenge between coral species

Exposure to stony coral tissue loss disease (SCTLD) in these experiments caused evident transcriptional responses in both coral species. In general, we observed a depression of host metabolic pathways and a corresponding increase in expression of stress response genes and nuclear processes (*Figure S2*). This is unsurprising given consistency in transcriptomic responses to myriad stressors, a phenomenon characterized as a conserved stress response among diverse coral taxa (Dixon et al., 2020; Wang et al., 2009). While there was evidence of a strong transcriptional response to disease exposure in host corals, there was little variation in the transcriptional response of symbionts in both experiments. This may be due to lower alignment rates to the symbiont transcriptomes relative to the coral hosts ($6.5 \pm 0.3\%$ for *Cladocopium* and $15.6 \pm 0.8\%$ for *Durusdinium* vs. $61.2 \pm 0.7\%$ for *M. cavernosa* and $60.3 \pm 1.6\%$ for *O. faveolata*, respectively) or comparatively poor annotations in symbiont references. Additional biological mechanisms may also explain the relatively weak symbiont gene expression signal, such as in hospite transcriptional stability (Barshis et al., 2014; Davies et al., 2018), host

suppression of symbiont transcription (Mohamed et al., 2020), or reliance on post-transcriptional regulation (Roy et al., 2018). Therefore, we have focused primarily on interpretation of the coral host datasets to minimize speculation with the symbiont datasets.

Through comparative analyses between coral species in the transmission experiment, we found consistent overlap in the majority of transcriptional responses following exposure to SCTLD. Notably, metabolic pathways were the most suppressed eukaryotic orthologous group (KOG) terms in diseased versus healthy samples for both species, while membrane structure, cell motility and defense mechanisms were often upregulated with exposure to disease (*Figure S2*). Of 681 differentially expressed genes (DEGs) and 21 gene ontology (GO) terms shared between *M. cavernosa* and *O. faveolata* (*Figures 2* and *3*), the majority of DEGs (~64%) and all GO terms were expressed or enriched in the same direction in response to SCTLD exposure, suggesting that there are many conserved pathways among coral species functioning in the same roles. This relationship has been corroborated in two recent studies by MacKnight et al. (2022) and Beavers et al. (2023), which examined transcriptional responses of several coral species (including our study species) to white plague disease and SCTLD, respectively. Both studies reported upregulation of immunity and cytoskeletal arrangement gene pathways following disease exposure across all species, with variation in intracellular protein trafficking pathways related to differences between disease susceptibility among and within species. Similarly, we observed higher enrichment of protein trafficking KOG and GO terms in diseased versus healthy *M. cavernosa*, which is less susceptible to SCTLD than *O. faveolata* (*Figure 3*; *Figure S2*; Meiling et al., 2021; NOAA, 2018).

Conversely, a minority of DEGs showed inverse relationships between species following exposure to SCTLD (*Figure 2*). For example, cytoskeletal structure and intracellular trafficking genes were strongly upregulated in *M. cavernosa* but suppressed in *O. faveolata*, and likely relate to differences in disease susceptibility as described above. The galactose binding lectin domain was upregulated in *O. faveolata* but strongly suppressed in *M. cavernosa* (*Figure 2b*). This pathway is especially important in recognition of glycan ligands on algal symbiont cell surfaces during initiation of symbiosis (Yoshioka et al., 2022), implying that losses of *Durusdinium* symbionts in *O. faveolata* were greater than *Cladocopium* in *M. cavernosa*, and indicate potential attempts at recovery of *in hospite* symbiont assemblages. Despite this variation in gene-level expression patterns spanning metabolic, transport and immune processes, functional enrichment of KOG and GO terms were largely similar between species (*Figure 3*; *Figure S2*), potentially indicating plasticity of conserved gene pathways between *M. cavernosa* and *O. faveolata* (i.e., distantly related species using the same gene pathways in different ways). This modulation may be indicative of plasticity related to disease susceptibility (e.g., Beavers et al., 2023; MacKnight et al., 2022), and warrants additional investigation with other species affected by SCTLD.

Both prior studies that examined transcriptomic responses to SCTLD (Beavers et al., 2023; Traylor-Knowles et al., 2021) identified

differentially expressed gene processes implicated in coral immunity following exposure to SCTLD. Here, we report significant variation of the same pathways in diseased individuals of both species (Figures S4–S6). Apoptosis, a well-known process implicated in cell death and necrosis (D'Arcy, 2019; Fuess et al., 2017), was naturally upregulated in diseased samples relative to healthy controls. Extracellular matrix genes were often downregulated following disease exposure in both species and are hypothesized to be related to wound healing and the prevention of lesion progression (Traylor-Knowles et al., 2021; Young et al., 2020). Transforming growth factor-beta (TGF- β) pathways are linked with increased microtubule and ciliary activity (Fuess et al., 2020; Traylor-Knowles et al., 2021), which we observed to be upregulated in diseased individuals across both experiments (Table S1; Figure S8). Ciliary action has been documented to help corals maintain their surface microbial layer which aids in pathogen removal (Gavish et al., 2021), and may be upregulated during immune challenge as a means of initial defense (Chang-sut et al., 2022). Nuclear factor kappa B (NF- κ B) genes were also upregulated in diseased versus healthy samples (Figures S5 and S6), where this transcription factor is well-known for its role in immune activation and potentially in regulation of the coral-algal symbiosis (Voolstra et al., 2009; Williams et al., 2018).

Similarly, Beavers et al. (2023) identified significant upregulation of Ras-related protein rab 7 (rab7) across five coral species exposed to SCTLD, which is a gene implicated in autophagy of zooxanthellae (Chen et al., 2003). The authors concluded that rab7 expression is an indicator of the breakdown of the coral-algal symbiosis in response to disease exposure, and therefore could be a useful bioindicator of SCTLD exposure. Rab7 was not found to be differentially expressed in any of our datasets, so we could not corroborate the pattern observed in the aforementioned study. Instead, we found the key members of WGCNA modules (i.e., module hub genes; Table S3) to be associated with known symbiosis and immune-related processes including mannose-6-phosphate receptor (Kvennefors et al., 2008; Rodriguez-Lanetty et al., 2009), scavenger receptor (Neubauer et al., 2016), and spondin2 (Kenkel et al., 2014). Taken together, expression of these pathways may be related to the hypothesis that SCTLD is caused by a virus targeting Symbiodiniaceae (Veglia et al., 2022; Work et al., 2021), but this observation requires further study.

Additional immune-related gene pathways were shown to be indicators of disease exposure and of the strong coral response to SCTLD exposure in this study. Peroxidases have been shown to be a component of the innate immune response to disease and thermal stress through their production of antibiotic compounds (Mydlarz & Harvell, 2007; Palmer, 2018); we identified 10 peroxidase genes with variable expression levels both within and between species, indicative of species-specific regulation of conserved pathways (Figures S5 and S6). Eight protein tyrosine kinase genes (PTKs) were mostly upregulated in diseased corals, which promote inflammatory responses to pathogens in corals (Fuess et al., 2016), corroborating that cytokine production plays a role in the response to

SCTLD exposure (Traylor-Knowles et al., 2021). One WD repeat gene was downregulated in diseased *O. faveolata* in the transmission experiment (Figures S5 and S6); this class of immune genes provides negative regulation of apoptotic and immune responses (Aranda et al., 2011), though their function in coral immunity is not well understood. The corroboration of conserved immune functions among species in this study and the only other transcriptomic resources related to SCTLD exposure at present (Beavers et al., 2023; Traylor-Knowles et al., 2021) provides evidence of their importance in the immune response to this disease, and further may be useful in the identification of biomarkers of disease exposure in wild corals (Traylor-Knowles et al., 2022).

Finally, similarities between no active infection (NAI) and healthy corals in GO enrichment analyses corroborated variance explained by PCoA ordination (Figure 1), suggesting that disease exposure does not necessarily result in a disease response at the transcriptomic level, and posits that innate resistance may be present in some individuals. This may be through immune front-loading (e.g., MacKnight et al., 2022), such as seen in the upregulation of cilium movement GO terms in NAI samples relative to healthy controls, which was also upregulated in diseased individuals. Downregulation of the endoplasmic reticulum lumen GO term in NAI samples, similar terms to which were conversely upregulated in diseased versus healthy and diseased versus NAI individuals (Tables S1 and S2), is likely an initial response to acute stress and may promote resistance to endoplasmic reticulum stress (such as protein misfolding or a breakdown of homeostasis; Aguilar et al., 2019; Aranda et al., 2011). There may also be inherent genetic resistance to disease in some genotypes (Vollmer & Kline, 2008), perhaps due to somatic age (Kelley et al., 2021; Ward, 2007), microbiome associations (MacKnight et al., 2021), or epigenetic processes (Thurber et al., 2020), and these potential relationships have only begun to be explored with SCTLD.

4.2 | Antibiotic treatment reverses transcriptional signatures of SCTLD

Treatment of corals with amoxicillin appears to result in a 'normalization' of host transcriptional pathways associated with the response to SCTLD, and to a lesser extent, of algal symbiont pathways. Treated corals were statistically indistinguishable from healthy controls and significantly different from their original diseased state (Figure 4), indicating a return to 'pre-disease' gene expression patterns. Comparisons of diseased versus healthy *M. cavernosa* across transmission and intervention experiments revealed mostly consistent patterns, with downregulation of metabolic pathways and upregulation of stress response, immune, and nuclear processes (Figure 5; Figure S10). The majority of shared DEGs between diseased individuals in both experiments were expressed in the same direction (~64%); however, following antibiotic treatment, the majority of shared DEGs (~76%, Figure S9) were inversely expressed relative to the pre-treatment

diseased state. Perhaps the most exciting conclusions are that this study provides compelling evidence of a reversal of the same transcriptomic mechanisms involved in the immune response to SCTLD following treatment with amoxicillin, and further, it proposes that targeted disease intervention may be beneficial to the coral beyond removal of potential pathogens and co-occurring opportunistic microbes. As studies evaluating the effectiveness of antibiotic treatments on diseased corals often focus on visible observations (i.e., lesion progression and/or quiescence; Forrester et al., 2022; Neely et al., 2020; Shilling et al., 2021; Walker et al., 2021) or shifts in microbial communities (Sweet et al., 2011, 2014) as a means of assessing treatment success, this hypothesis requires further testing to elucidate the long-term impacts of antibiotic treatment on other members of the holobiont including the coral host. For example, antibiotics have additional immune-modulating and anti-inflammatory impacts on humans beyond alteration of associated microbial communities (Pradhan et al., 2016), which may prove beneficial to corals affected by SCTLD. Likewise, the implications of antibiotic treatment on associated Symbiodiniaceae assemblages in corals (Connelly et al., 2022), including a depression of nuclear processes reported here (Figure 5), are mostly unknown but may also impact holobiont health.

Examination of SCTLD-associated immune responses (Beavers et al., 2023; Traylor-Knowles et al., 2021) in the intervention experiment reinforced the reversal of transcriptional patterns following amoxicillin treatment. PTK and WD repeat genes had significant variation in expression between diseased corals and healthy controls, and in some cases, between diseased and treated corals (Figure S7). In two of those cases (non-membrane spanning PTK activity and WD repeat-containing protein 37), expression in treated individuals was also significantly higher than that in healthy controls, perhaps as a form of overcompensation during an attempt at recovery from prior disease exposure. A heat shock protein family gene was also identified as a hub gene in weighted gene coexpression network analysis (WGCNA) in *M. cavernosa*, demonstrating a negative correlation with treated corals relative to diseased corals (Figure 6). Heat shock proteins are considered a key component of the general coral stress response (Dixon et al., 2020), and its downregulation following antibiotic treatment implies a reduction in the stress response by the coral host.

At the gene functional pathway level, GO terms associated with activation of the NF- κ B pathway (ubiquitin; Beavers et al., 2023) that were upregulated in diseased versus healthy corals in the intervention experiment were notably absent following antibiotic treatment, suggesting that the downstream NF- κ B immune response was no longer active (Figure S8). Suppression of oxidoreductase GO terms, as seen in diseased relative to healthy corals in the intervention experiment, has been shown to be a sign of redox homeostasis dysfunction (Williams et al., 2021), possibly making disease-affected corals more susceptible to oxygen stress and reactive oxygen species (ROS). Following antibiotic treatment, those pathways were upregulated, indicating the potential for re-establishment of homeostasis (Figure S8).

4.3 | Transcriptomics provide support for targeted antibiotic treatment as an effective SCTLD intervention approach

Amoxicillin is effective at slowing or halting SCTLD lesion progression on individual colonies, including in field settings (Forrester et al., 2022; Neely et al., 2020; Shilling et al., 2021; Walker et al., 2021). Here, we provide the first transcriptomic evidence that antibiotic intervention is indeed successful in promoting coral recovery from SCTLD, and may even provide additional direct benefits to coral immune processes beyond removal of pathogens alone. There are, however, multiple limitations of antibiotic treatment effectiveness on broad-scale disease intervention efforts, including that this approach often requires multiple re-treatments, requires continuous monitoring, and is labour-intensive (Neely et al., 2020; Walker et al., 2021). While application of amoxicillin shows a high rate of success (~95%) in halting individual lesions, it does not necessarily prevent the formation of new lesions on a treated colony through time (Neely et al., 2020; Shilling et al., 2021). It also remains to be tested how long the ‘normalization’ of coral transcription, and particularly immune responses, remains in antibiotic-treated corals, and whether treatment may provide additional benefits or long-term consequences. We show that antibiotic treatment may stimulate immune responses (Figure S7), which is generally energetically costly, and has been shown to cause reduced fecundity in corals affected by a disease broadly characterized as growth anomalies (reviewed in Ricci et al., 2022). Finally, it is currently unknown what impacts antibiotic application may have on diverse coral reef ecosystems beyond the coral host, notably potential antibiotic resistance in microbial communities (Griffin et al., 2020; Liu et al., 2020). Antibiotic treatment may additionally have negative impacts on healthy coral microbiomes, potentially increasing susceptibility of corals to other stressors such as elevated temperatures (Connelly et al., 2022).

Alternative treatment methods are therefore warranted for further investigation with multi-‘omic approaches in the mitigation of SCTLD, as well as future coral disease outbreaks. In particular, probiotic treatments are gaining research interest due to their potential benefits to coral survival following disease exposure (Peixoto et al., 2021), thermal stress (Doering et al., 2021; Santoro et al., 2021), and exposure to pollutants (Silva et al., 2021). Probiotic treatments are in development for SCTLD (Deutsch et al., 2022), and field trials are necessary to assess treatment effectiveness in a reef environment (Peixoto et al., 2021). Phage therapy also shows promise for the treatment of bacterial pathogens that affect corals (Jacquemot et al., 2018; Teplitski & Ritchie, 2009; Thurber et al., 2020), but many of these approaches are not yet fully operational. Potential impacts of these alternative treatment approaches on coral immunity are also unknown.

While treatment of individual coral colonies with antibiotics is not intended to be a long-term solution to curbing the spread of SCTLD, it may represent a feasible method of mitigating impacts on high-value conservation and restoration targets, particularly ecologically important, rare, and reproductively viable members of the

population. This is of particular importance while disease diagnostics are still being developed for SCTLD and other diseases. Disease diagnostics, when operational and scalable, may instead allow broad mitigation of pathogen transport via disease vectors and sources, potentially eliminating the need for colony-level disease intervention. Continued examination of gene mechanisms and functions will also improve understanding of coral immune responses (Traylor-Knowles et al., 2022), facilitating targeted treatment approaches in future disease outbreaks. Disease response efforts focusing on identification and diagnosis, mitigation of spread, and treatment of affected individuals require a holistic understanding of coral immunity and resilience at the individual level in order to maximize conservation and restoration success at the population level.

5 | CONCLUSIONS

Through complementary studies examining the transcriptomic responses of corals to stony coral tissue loss disease (SCTLD) and subsequent antibiotic treatment, we identified a consistent signature of immune responses in both coral species examined. Furthermore, we observed evidence of a reversal in immune and metabolic responses related to disease exposure when corals were treated with amoxicillin, suggestive of a recovery process occurring at the host level. The strong impacts of antibiotic treatment on coral transcription, both in terms of a return to 'healthy' levels, and in some cases promotion of immune activation beyond levels seen in healthy controls, are suggestive of direct benefits of antibiotic exposure to the coral host. This phenomenon may, in part, explain why antibiotics appear to be effective in slowing or halting SCTLD lesions, particularly if the disease is caused by a viral pathogen or pathogenic consortium containing viruses. If indeed SCTLD is caused by a virus targeting Symbiodiniaceae as has been hypothesized (Veglia et al., 2022; Work et al., 2021), the stabilization of the coral-algal symbiosis through coral immune activation and metabolic support may be of the utmost importance in determining the survival of the holobiont.

AUTHOR CONTRIBUTIONS

Michael S. Studivan: Conceptualization, Funding Acquisition, Methodology, Investigation, Statistical Analysis, Data Curation, Writing-Original Draft, Writing-Review & Editing. **Ryan J. Eckert:** Methodology, Investigation, Writing-Review & Editing. **Erin Shilling:** Conceptualization, Methodology, Investigation, Writing-Review & Editing. **Nash Soderberg:** Methodology, Investigation, Writing-Review & Editing. **Ian C. Enochs:** Funding Acquisition, Methodology, Writing-Review & Editing. **Joshua D. Voss:** Conceptualization, Funding Acquisition, Methodology, Investigation, Writing-Review & Editing.

ACKNOWLEDGEMENTS

We acknowledge Victoria Barker, Emily Osborne, and Katharine Egan for programmatic support in the development of this study, and Ian Combs and Matt Roy for assistance in field sampling. Coral colonies were monitored, sampled, and treated under permits from

the Florida Fish and Wildlife Conservation Commission to Joshua Voss (Special Activity Licenses SAL-19-1702-SRP and SAL-19-2022-SRP). High-performance computing was provided by Research Computing Services at Florida Atlantic University. This study was funded by the NOAA OAR 'Omics Program to Joshua Voss and Michael Studivan, with additional funding support from the Florida Department of Environmental Protection to Joshua Voss (B55008) and the NOAA Coral Reef Conservation Program to Ian Enochs and Michael Studivan (#31252). This is contribution 2316 from Harbor Branch Oceanographic Institute at Florida Atlantic University.

CONFLICT OF INTEREST STATEMENT

All authors declare that they have no conflicts of interest.

OPEN RESEARCH BADGES



This article has earned an Open Data badge for making publicly available the digitally-shareable data necessary to reproduce the reported results. The data is available at <https://www.ncbi.nlm.nih.gov/bioproject/PRJNA897845>.

DATA AVAILABILITY STATEMENT

All sequence files associated with this study can be found in the National Center for Biotechnology Information (NCBI) Sequence Read Archive (SRA) under BioProject [PRJNA897845](https://www.ncbi.nlm.nih.gov/bioproject/PRJNA897845), accession numbers SAMN31581862 through SAMN31582010. Datasets and analysis scripts generated from this study are available in a GitHub repository (Studivan, 2023). Pipelines for bioinformatics and transcriptome annotations are described in separate GitHub repositories for Tag-Seq, *M. cavernosa*, and *O. faveolata* (Studivan, 2022a, 2022b, 2022c).

BENEFIT-SHARING STATEMENT

Benefits from this research accrue from the sharing of our data and results on public databases as described above, and through the Florida Department of Environmental Protection's Disturbance Advisory Committee.

ORCID

- Michael S. Studivan <https://orcid.org/0000-0002-3771-0415>
Ryan J. Eckert <https://orcid.org/0000-0002-3010-9395>
Erin Shilling <https://orcid.org/0000-0003-1026-6892>
Nash Soderberg <https://orcid.org/0000-0002-3155-4167>
Ian C. Enochs <https://orcid.org/0000-0002-8867-0361>
Joshua D. Voss <https://orcid.org/0000-0002-0653-2767>

REFERENCES

- Abey, G. S., Ushijima, B., Bartels, E., Walter, C., Kuehl, J., Jones, S., & Paul, V. J. (2021). Changing stony coral tissue loss disease dynamics through time in *Montastraea cavernosa*. *Frontiers in Marine Science*, 8, 699075. <https://doi.org/10.3389/fmars.2021.699075>
Abey, G. S., Ushijima, B., Campbell, J. E., Jones, S., Williams, G. J., Meyer, J. L., Häse, C., & Paul, V. J. (2019). Pathogenesis of a tissue loss disease affecting multiple species of corals along the Florida Reef

- Tract. *Frontiers in Marine Science*, 6, 00678. <https://doi.org/10.3389/fmars.2019.00678>
- Aguilar, C., Raina, J. B., Fôret, S., Hayward, D. C., Lapeyre, B., Bourne, D. G., & Miller, D. J. (2019). Transcriptomic analysis reveals protein homeostasis breakdown in the coral *Acropora millepora* during hypersaline stress. *BMC Genomics*, 20(1), 148. <https://doi.org/10.1186/s12864-019-5527-2>
- Aranda, M., Banaszak, A. T., Bayer, T., Luyten, J. R., Medina, M., & Voolstra, C. R. (2011). Differential sensitivity of coral larvae to natural levels of ultraviolet radiation during the onset of larval competence. *Molecular Ecology*, 20(14), 2955–2972. <https://doi.org/10.1111/j.1365-294X.2011.05153.x>
- Barshis, D. J., Ladner, J. T., Oliver, T. A., & Palumbi, S. R. (2014). Lineage-specific transcriptional profiles of *Symbiodinium* spp. unaltered by heat stress in a coral host. *Molecular Biology and Evolution*, 31(6), 1343–1352. <https://doi.org/10.1093/molbev/msu107>
- Beavers, K. M., Van Buren, E. W., Rossin, A. M., Emery, M. A., Veglia, A. J., Kerrick, C. E., MacKnight, N. J., Dimos, B. A., Meiling, S. S., Smith, T. B., Apprill, A., Muller, E. M., Holstein, D. M., Correa, A. M. S., Brandt, M. E., & Mydlarz, L. D. (2023). Stony coral tissue loss disease induces transcriptional signatures of in situ degradation of dysfunctional Symbiodiniaceae. *Nature Communications*, 14(1), 2915. <https://doi.org/10.1038/s41467-023-38612-4>
- Becker, C. C., Brandt, M., Miller, C. A., & Apprill, A. (2021). Microbial bioindicators of stony coral tissue loss disease identified in corals and overlying waters using a rapid field-based sequencing approach. *Environmental Microbiology*, 24, 1166–1182. <https://doi.org/10.1111/1462-2920.15718>
- Changsut, I., Womack, H. R., Shickle, A., Sharp, K. H., & Fuess, L. E. (2022). Variation in symbiont density is linked to changes in constitutive immunity in the facultatively symbiotic coral, *Astrangia poculata*. *Biology Letters*, 18(11), 20220273. <https://doi.org/10.1098/rsbl.2022.0273>
- Chen, H., & Boutros, P. C. (2011). VennDiagram: A package for the generation of highly-customizable Venn and Euler diagrams in R. *BMC Bioinformatics*, 12, 35. <https://doi.org/10.1186/1471-2105-12-35>
- Chen, M.-C., Cheng, Y.-M., Sung, P.-J., Kuo, C.-E., & Fang, L.-S. (2003). Molecular identification of Rab7 (ApRab7) in *Aiptasia pulchella* and its exclusion from phagosomes harboring zooxanthellae. *Biochemical and Biophysical Research Communications*, 308(3), 586–595. [https://doi.org/10.1016/S0006-291X\(03\)01428-1](https://doi.org/10.1016/S0006-291X(03)01428-1)
- Combs, I. R., Studivan, M. S., Eckert, R. J., & Voss, J. D. (2021). Quantifying impacts of stony coral tissue loss disease on corals in Southeast Florida through surveys and 3D photogrammetry. *PLoS One*, 16(6), e0252593. <https://doi.org/10.1371/journal.pone.0252593>
- Connelly, M. T., McRae, C. J., Liu, P.-J., Martin, C. E., & Traylor-Knowles, N. (2022). Antibiotics alter *Pocillopora* coral-Symbiodiniaceae-bacteria interactions and cause microbial dysbiosis during heat stress. *Frontiers in Marine Science*, 8, 814124. <https://doi.org/10.3389/fmars.2021.814124>
- D'Arcy, M. S. (2019). Cell death: A review of the major forms of apoptosis, necrosis and autophagy. *Cell Biology International*, 43, 582–592. <https://doi.org/10.1002/cbin.11137>
- Danecek, P., Bonfield, J. K., Liddle, J., Marshall, J., Ohan, V., Pollard, M. O., Whitwham, A., Keane, T., McCarthy, S. A., Davies, R. M., & Li, H. (2021). Twelve years of SAMtools and BCFtools. *GigaScience*, 10(2). <https://doi.org/10.1093/gigascience/giab008>
- Davies, S. W., Ries, J. B., Marchetti, A., & Castillo, K. D. (2018). *Symbiodinium* functional diversity in the coral *Siderastrea siderea* is influenced by thermal stress and reef environment, but not ocean acidification. *Frontiers in Marine Science*, 5, 150. <https://doi.org/10.3389/fmars.2018.00150>
- Deutsch, J. M., Jaiyesimi, O. A., Pitts, K. A., Houk, J., Ushijima, B., Walker, B. K., Paul, V. J., & Garg, N. (2021). Metabolomics of healthy and stony coral tissue loss disease affected *Montastraea cavernosa* corals. *Frontiers in Marine Science*, 8, 714778. <https://doi.org/10.3389/fmars.2021.714778>
- Deutsch, J. M., Mandelare-Ruiz, P., Yang, Y., Foster, G., Routhu, A., Houk, J., De La Flor, Y. T., Ushijima, B., Meyer, J. L., Paul, V. J., & Garg, N. (2022). Metabolomics approaches to derePLICATE natural products from coral-derived bioactive bacteria. *Journal of Natural Products*, 85, 462–478. <https://doi.org/10.1021/acs.jnatprod.1c01110>
- Dixon, G., Abbott, E., & Matz, M. V. (2020). Meta-analysis of the general coral stress response: *Acropora* corals show opposing responses depending on stress intensity. *Molecular Ecology*, 29, 2855–2870. <https://doi.org/10.1111/mec.15535>
- Dixon, G. B., Davies, S. W., Aglyamova, G. A., Meyer, E., Bay, L. K., & Matz, M. V. (2015). Genomic determinants of coral heat tolerance across latitudes. *Science*, 348, 1460–1462. <https://doi.org/10.1126/science.1261224>
- Doering, T., Wall, M., Putchim, L., Rattanawongwan, T., Schroeder, R., Hentschel, U., & Roik, A. (2021). Towards enhancing coral heat tolerance: A "microbiome transplantation" treatment using inoculations of homogenized coral tissues. *Microbiome*, 9, 102. <https://doi.org/10.1186/s40168-021-01053-6>
- Emms, D. M., & Kelly, S. (2015). OrthoFinder: Solving fundamental biases in whole genome comparisons dramatically improves orthogroup inference accuracy. *Genome Biology*, 16, 157. <https://doi.org/10.1186/s13059-015-0721-2>
- Emms, D. M., & Kelly, S. (2019). OrthoFinder: Phylogenetic orthology inference for comparative genomics. *Genome Biology*, 20, 238. <https://doi.org/10.1186/s13059-019-1832-y>
- Forrester, G. E., Arton, L., Horton, A., Nickles, K., & Forrester, L. M. (2022). Antibiotic treatment ameliorates the impact of stony coral tissue loss disease (SCTLD) on coral communities. *Frontiers in Marine Science*, 9, 859740. <https://doi.org/10.3389/fmars.2022.859740>
- Fuess, L. E., Butler, C. C., Brandt, M. E., & Mydlarz, L. D. (2020). Investigating the roles of transforming growth factor-beta in immune response of *Orcicella faveolata*, a scleractinian coral. *Developmental and Comparative Immunology*, 107, 103639. <https://doi.org/10.1016/j.dci.2020.103639>
- Fuess, L. E., Pinzón C. J. H., Weil, E., Grinshpon, R. D., & Mydlarz, L. D. (2017). Life or death: Disease-tolerant coral species activate autophaagy following immune challenge. *Proceedings of the Royal Society B: Biological Sciences*, 284, 20170771. <https://doi.org/10.1098/rspb.2017.0771>
- Fuess, L. E., Pinzón C. J. H., Weil, E., & Mydlarz, L. D. (2016). Associations between transcriptional changes and protein phenotypes provide insights into immune regulation in corals. *Developmental and Comparative Immunology*, 62, 17–28. <https://doi.org/10.1016/j.dci.2016.04.017>
- Gavish, A. R., Shapiro, O. H., Kramarsky-Winter, E., & Vardi, A. (2021). Microscale tracking of coral-vibrio interactions. *ISME Communications*, 1(1), 18. <https://doi.org/10.1038/s43705-021-00016-0>
- González-Barrios, F. J., & Álvarez-Filip, L. (2018). A framework for measuring coral species-specific contribution to reef functioning in the Caribbean. *Ecological Indicators*, 95, 877–886. <https://doi.org/10.1016/j.ecolind.2018.08.038>
- Gordon, A., & Hannon, G. (2010). Fastx-toolkit. FASTQ/A short-reads preprocessing tools (unpublished), 5. http://hannonlab.cshl.edu/fastx_toolkit
- Griffin, D. W., Banks, K., Gregg, K., Shedler, S., & Walker, B. K. (2020). Antibiotic resistance in marine microbial communities proximal to a Florida sewage outfall system. *Antibiotics*, 9, 118. <https://doi.org/10.3390/antibiotics9030118>
- Hadfield, J. D. (2010). MCMCglmm: MCMC methods for multi-response GLMMs in R. *Journal of Statistical Software*, 33(2), 1–22. <https://doi.org/10.18637/jss.v033.i02>
- Huerta-Cepas, J., Forslund, K., Coelho, L. P., Szklarczyk, D., Jensen, L. J., Von Mering, C., & Bork, P. (2018). Fast genome-wide functional

- annotation through orthology assignment by eggNOG-Mapper. *Molecular Biology and Evolution*, 34, 2115–2122. <https://doi.org/10.1093/molbev/msx148>
- Huerta-Cepas, J., Szklarczyk, D., Forslund, K., Cook, H., Heller, D., Walter, M. C., Rattei, T., Mende, D. R., Sunagawa, S., Kuhn, M., Jensen, L. J., Von Mering, C., & Bork, P. (2016). eggNOG 4.5: A hierarchical orthology framework with improved functional annotations for eukaryotic, prokaryotic and viral sequences. *Nucleic Acids Research*, 44, D286–D293. <https://doi.org/10.1093/nar/gkv1248>
- Huntley, N., Brandt, M. E., Becker, C. C., Miller, C. A., Meiling, S. S., Correa, A. M. S., Holstein, D. M., Muller, E. M., Mydlarz, L. D., Smith, T. B., & Apprill, A. (2022). Experimental transmission of stony coral tissue loss disease results in differential microbial responses within coral mucus and tissue. *ISME Communications*, 2(1), 46. <https://doi.org/10.1038/s43705-022-00126-3>
- Jacquemot, L., Bettarel, Y., Monjol, J., Corre, E., Halary, S., Desnues, C., Bouvier, T., Ferrier-Pagès, C., & Baudoux, A.-C. (2018). Therapeutic potential of a new jumbo phage that infects *Vibrio coralliilyticus*, a widespread coral pathogen. *Frontiers in Microbiology*, 9, 2501. <https://doi.org/10.3389/fmicb.2018.02501>
- Jombart, T. (2008). adegenet: A R package for the multivariate analysis of genetic markers. *Bioinformatics*, 24(11), 1403–1405. <https://doi.org/10.1093/bioinformatics/btn129>
- Kassambara, A., Kosinski, M., & Biecek, P. (2021). *Survminer: Drawing survival curves using "ggplot2"*. R package version 0.4.9.
- Kauffmann, A., Gentleman, R., & Huber, W. (2009). *arrayQualityMetrics*—A bioconductor package for quality assessment of microarray data. *Bioinformatics*, 25(3), 415–416. <https://doi.org/10.1093/bioinformatics/btn647>
- Kelley, E. R., Sleith, R. S., Matz, M. V., & Wright, R. M. (2021). Gene expression associated with disease resistance and long-term growth in a reef-building coral. *Royal Society Open Science*, 8(4), 210113. <https://doi.org/10.1098/rsos.210113>
- Kenkel, C. D., Sheridan, C., Leal, M. C., Bhagooli, R., Castillo, K. D., Kurata, N., McGinty, E., Goulet, T. L., & Matz, M. V. (2014). Diagnostic gene expression biomarkers of coral thermal stress. *Molecular Ecology Resources*, 14(4), 667–678. <https://doi.org/10.1111/1755-0998.12218>
- Kitchen, S. A., Crowder, C. M., Poole, A. Z., Weis, V. M., & Meyer, E. (2015). De novo assembly and characterization of four anthozoan (Phylum Cnidaria) transcriptomes. *G3: Genes, Genomes, Genetics*, 5, 2441–2452. <https://doi.org/10.1534/g3.115.020164>
- Kolde, R. (2019). *Pheatmap: Pretty heatmaps*. R package version 1.0.12.
- Koval, G., Rivas, N., D'Alessandro, M., Hesley, D., Santos, R., & Lirman, D. (2020). Fish predation hinders the success of coral restoration efforts using fragmented massive corals. *PeerJ*, 8, e9978. <https://doi.org/10.7717/peerj.9978>
- Kramer, P. R., Roth, L., & Lang, J. (2019). *Map of stony coral tissue loss disease outbreak in the Caribbean*. ArcGIS online. www.agrra.org
- Kvennfors, E. C. E., Leggat, W., Hoegh-Guldberg, O., Degnan, B. M., & Barnes, A. C. (2008). An ancient and variable mannose-binding lectin from the coral *Acropora millepora* binds both pathogens and symbionts. *Developmental & Comparative Immunology*, 32(12), 1582–1592. <https://doi.org/10.1016/j.dci.2008.05.010>
- Landsberg, J. H., Kiryu, Y., Peters, E. C., Wilson, P. W., Perry, N., Waters, Y., Maxwell, K. E., Huebner, L. K., & Work, T. M. (2020). Stony coral tissue loss disease in Florida is associated with disruption of host-zooxanthellae physiology. *Frontiers in Marine Science*, 7, 576013. <https://doi.org/10.3389/fmars.2020.576013>
- Langfelder, P., & Horvath, S. (2008). WGCNA: An R package for weighted correlation network analysis. *BMC Bioinformatics*, 9, 559. <https://doi.org/10.1186/1471-2105-9-559>
- Langmead, B., & Salzberg, S. L. (2012). Fast gapped-read alignment with Bowtie 2. *Nature Methods*, 9, 357–359. <https://doi.org/10.1038/nmeth.1923>
- Liu, S., Su, H., Pan, Y.-F., & Xu, X.-R. (2020). Spatial and seasonal variations of antibiotics and antibiotic resistance genes and ecological risks in the coral reef regions adjacent to two typical islands in South China Sea. *Marine Pollution Bulletin*, 158, 111424. <https://doi.org/10.1016/j.marpolbul.2020.111424>
- Love, M. I., Huber, W., & Anders, S. (2014). Moderated estimation of fold change and dispersion for RNA-seq data with DESeq2. *Genome Biology*, 15, 550–571. <https://doi.org/10.1186/s13059-014-0550-8>
- MacKnight, N. J., Cobleigh, K., Lasseigne, D., Chaves-Fonnegra, A., Gutting, A., Dimos, B., Antoine, J., Fuess, L., Ricci, C., Butler, C., Muller, E. M., Mydlarz, L. D., & Brandt, M. (2021). Microbial dysbiosis reflects disease resistance in diverse coral species. *Communications Biology*, 4(1), 679. <https://doi.org/10.1038/s42003-021-02163-5>
- MacKnight, N. J., Dimos, B. A., Beavers, K. M., Muller, E. M., Brandt, M. E., & Mydlarz, L. D. (2022). Disease resistance in coral is mediated by distinct adaptive and plastic gene expression profiles. *Science Advances*, 8, eab6153. <https://doi.org/10.1126/sciadv.abo6153>
- Meiling, S. S., Muller, E. M., Lasseigne, D., Rossin, A., Veglia, A. J., MacKnight, N., Dimos, B., Huntley, N., Correa, A. M. S., Smith, T. B., Holstein, D. M., Mydlarz, L. D., Apprill, A., Brandt, M. E., & Neely, K. L. (2021). Variable species responses to experimental stony coral tissue loss disease (SCTLD) exposure. *Frontiers in Marine Science*, 8, 670829. <https://doi.org/10.3389/fmars.2021.670829>
- Meyer, J. L., Castellanos-Gell, J., Aeby, G. S., Häse, C. C., Ushijima, B., & Paul, V. J. (2019). Microbial community shifts associated with the ongoing stony coral tissue loss disease outbreak on the Florida Reef Tract. *Frontiers in Microbiology*, 10, 2244. <https://doi.org/10.3389/fmicb.2019.02244>
- Mohamed, A. R., Andrade, N., Moya, A., Chan, C. X., Negri, A. P., Bourne, D. G., Ying, H., Ball, E. E., & Miller, D. J. (2020). Dual RNA-sequencing analyses of a coral and its native symbiont during the establishment of symbiosis. *Molecular Ecology*, 29(20), 3921–3937. <https://doi.org/10.1111/mec.15612>
- Mydlarz, L. D., & Harvell, C. D. (2007). Peroxidase activity and inducibility in the sea fan coral exposed to a fungal pathogen. *Comparative Biochemistry and Physiology Part A: Molecular & Integrative Physiology*, 146, 54–62. <https://doi.org/10.1016/j.cbpa.2006.09.005>
- Neely, K. L., Macaulay, K. A., Hower, E. K., & Dobler, M. A. (2020). Effectiveness of topical antibiotics in treating corals affected by stony coral tissue loss disease. *PeerJ*, 8, 9289. <https://doi.org/10.7717/peerj.9289>
- Neubauer, E. F., Poole, A. Z., Detournay, O., Weis, V. M., & Davy, S. K. (2016). The scavenger receptor repertoire in six cnidarian species and its putative role in cnidarian-dinoflagellate symbiosis. *PeerJ*, 4, e2692. <https://doi.org/10.7717/peerj.2692>
- NOAA. (2018). *Stony coral tissue loss disease case definition* (p. 10). NOAA.
- Oksanen, J., Blanchet, F. G., Kindt, R., Legendre, P., Minchin, P. R., O'Hara, R., Simpson, G., Solymos, P., Stevens, M., & Wagner, H. (2015). *Vegan: Community ecology package*. R package version 2.0-10.
- Palmer, C. V. (2018). Warmer water affects immunity of a tolerant reef coral. *Frontiers in Marine Science*, 5, 253. <https://doi.org/10.3389/fmars.2018.00253>
- Paysan-Lafosse, T., Blum, M., Chuguransky, S., Grego, T., Pinto, B. L., Salazar, G. A., Bileschi, M. L., Bork, P., Bridge, A., Colwell, L., Gough, J., Haft, D. H., Letunić, I., Marchler-Bauer, A., Mi, H., Natale, D. A., Orengo, C. A., Pandurangan, A. P., Rivoire, C., ... Bateman, A. (2023). InterPro in 2022. *Nucleic Acids Research*, 51(D1), D418–D427. <https://doi.org/10.1093/nar/gkac993>
- Peixoto, R. S., Sweet, M., Villela, H. D. M., Cardoso, P., Thomas, T., Voolstra, C. R., Høj, L., & Bourne, D. G. (2021). Coral probiotics: Premise, promise, prospects. *Annual Review of Animal Biosciences*, 9, 265–288. <https://doi.org/10.1146/annurev-animal-090120-115444>
- Pinzón, J. H., Kamel, B., Burge, C. A., Harvell, C. D., Medina, M., Weil, E., & Mydlarz, L. D. (2015). Whole transcriptome analysis reveals

- changes in expression of immune-related genes during and after bleaching in a reef-building coral. *Royal Society Open Science*, 2, 140214. <https://doi.org/10.1098/rsos.140214>
- Pradhan, S., Madke, B., Kabra, P., & Singh, A. L. (2016). Anti-inflammatory and immunomodulatory effects of antibiotics and their use in dermatology. *Indian Journal of Dermatology*, 61, 469–481. <https://doi.org/10.4103/0019-5154.190105>
- Precht, W. F., Ginter, B. E., Robbart, M. L., Fura, R., & Van Woesik, R. (2016). Unprecedented disease-related coral mortality in Southeastern Florida. *Scientific Reports*, 6, 31374. <https://doi.org/10.1038/srep31374>
- R Core Team. (2021). *R: A language and environment for statistical computing*. R Foundation for Statistical Computing [Computer software]. <https://www.r-project.org/>
- Ricci, F., Leggat, W., Page, C. E., & Ainsworth, T. D. (2022). Coral growth anomalies, neoplasms, and tumors in the Anthropocene. *Trends in Microbiology*, 30(12), 1160–1173. <https://doi.org/10.1016/j.tim.2022.05.013>
- Rivas, N., Hesley, D., Kaufman, M., Unsworth, J., D'Alessandro, M., & Lirman, D. (2021). Developing best practices for the restoration of massive corals and the mitigation of predation impacts: Influences of physical protection, colony size, and genotype on outplant mortality. *Coral Reefs*, 40, 1227–1241. <https://doi.org/10.1007/s00338-021-02127-5>
- Rodriguez-Lanetty, M., Harii, S., & Hoegh-Guldberg, O. (2009). Early molecular responses of coral larvae to hyperthermal stress. *Molecular Ecology*, 18(24), 5101–5114. <https://doi.org/10.1111/j.1365-294X.2009.04419.x>
- Rosales, S. M., Clark, A. S., Huebner, L. K., Ruzicka, R. R., & Muller, E. M. (2020). Rhodobacterales and Rhizobiales are associated with stony coral tissue loss disease and its suspected sources of transmission. *Frontiers in Microbiology*, 11, 681. <https://doi.org/10.3389/fmicb.2020.00681>
- Rosales, S. M., Huebner, L. K., Clark, A. S., McMinds, R., Ruzicka, R. R., & Muller, E. M. (2022). Bacterial metabolic potential and micro-eukaryotes enriched in stony coral tissue loss disease lesions. *Frontiers in Marine Science*, 8, 776859. <https://doi.org/10.3389/fmars.2021.776859>
- Rosales, S. M., Huebner, L. K., Clark, A. S., Apprill, A., Baker, A. C., Becker, C. C., Bellantuono, A. J., Brandt, M. E., Clark, A. S., del Campo, J., Dennison, C. E., Eaton, K. R., Huntley, N. E., Kellogg, C. A., Medina, M., Meyer, J. L., Muller, E. M., Rodriguez-Lanetty, M., Salerno, J. L., ... Voss, J. D. (2023). A meta-analysis of the stony coral tissue loss disease microbiome finds key bacteria in unaffected and lesion tissue in diseased colonies. *ISME Communications*, 3(1), 19. <https://doi.org/10.1038/s43705-023-00220-0>
- Roy, S., Jagus, R., & Morse, D. (2018). Translation and translational control in dinoflagellates. *Microorganisms*, 6(2), 30. <https://doi.org/10.3390/microorganisms6020030>
- Santoro, E. P., Borges, R. M., Espinoza, J. L., Freire, M., Messias, C. S. M. A., Villela, H. D. M., Pereira, L. M., Vilela, C. L. S., Rosado, J. G., Cardoso, P. M., Rosado, P. M., Assis, J. M., Duarte, G. A. S., Perna, G., Rosado, A. S., Macrae, A., Dupont, C. L., Nelson, K. E., Sweet, M. J., ... Peixoto, R. S. (2021). Coral microbiome manipulation elicits metabolic and genetic restructuring to mitigate heat stress and evade mortality. *Science Advances*, 7, eabg3088. <https://doi.org/10.1126/sciadv.abg3088>
- Shilling, E. N., Combs, I. R., & Voss, J. D. (2021). Assessing the effectiveness of two intervention methods for stony coral tissue loss disease on *Montastraea cavernosa*. *Scientific Reports*, 11, 8566. <https://doi.org/10.1038/s41598-021-86926-4>
- Shoguchi, E., Beedessee, G., Hisata, K., Tada, I., Narisoko, H., Satoh, N., Kawachi, M., & Shintzato, C. (2021). A new dinoflagellate genome illuminates a conserved gene cluster involved in sunscreen biosynthesis. *Genome Biology and Evolution*, 13, evaa235. <https://doi.org/10.1093/gbe/evaa235>
- Silva, D. P., Villela, H. D. M., Santos, H. F., Duarte, G. A. S., Ribeiro, J. R., Ghizelini, A. M., Vilela, C. L. S., Rosado, P. M., Fazolato, C. S., Santoro, E. P., Carmo, F. L., Ximenes, D. S., Soriano, A. U., Rachid, C. T. C. C., Vega Thurber, R. L., & Peixoto, R. S. (2021). Multi-domain probiotic consortium as an alternative to chemical remediation of oil spills at coral reefs and adjacent sites. *Microbiome*, 9, 118. <https://doi.org/10.1186/s40168-021-01041-w>
- Studivan, M. S. (2022a). Mstudiva/Mcav-Cladocopium-annotated-transcriptome: Transcriptome annotations for *Montastraea cavernosa* and *Cladocopium* spp. (version 3.0). Zenodo. <https://doi.org/10.5281/zenodo.7007997>
- Studivan, M. S. (2022b). Mstudiva/Ofav-Durusdinum-annotated-transcriptome: Transcriptome annotations for *Orcicella faveolata* and *Durusdinum* spp. (version 1.0). Zenodo. <https://doi.org/10.5281/zenodo.7007995>
- Studivan, M. S. (2022c). mstudiva/tag-based_RNAseq: RNA extraction and Tag-Seq library preparation and analysis pipeline (version 1.0). Zenodo. <https://doi.org/10.5281/zenodo.7007692>
- Studivan, M. S. (2023). mstudiva/SCTLD-intervention-transcriptomics: Stony coral tissue loss disease transmission and antibiotic intervention transcriptomics (version 2.0). Zenodo. <https://doi.org/10.5281/zenodo.7998715>
- Studivan, M. S., Rossin, A. M., Rubin, E., Soderberg, N., Holstein, D. M., & Enochs, I. C. (2022). Reef sediments can act as a stony coral tissue loss disease vector. *Frontiers in Marine Science*, 8, 815698. <https://doi.org/10.3389/fmars.2021.815698>
- Sweet, M. J., Croquer, A., & Bythell, J. C. (2011). Dynamics of bacterial community development in the reef coral *Acropora muricata* following experimental antibiotic treatment. *Coral Reefs*, 30, 1121–1133. <https://doi.org/10.1007/s00338-011-0800-0>
- Sweet, M. J., Croquer, A., & Bythell, J. C. (2014). Experimental antibiotic treatment identifies potential pathogens of white band disease in the endangered Caribbean coral *Acropora cervicornis*. *Proceedings of the Royal Society B: Biological Sciences*, 281, 20140094. <https://doi.org/10.1098/rspb.2014.0094>
- Teplitski, M., & Ritchie, K. (2009). How feasible is the biological control of coral diseases? *Trends in Ecology & Evolution*, 24, 378–385. <https://doi.org/10.1016/j.tree.2009.02.008>
- Therneau, T. M. (2021). *Survival: A package for survival analysis in R*. R package version 3.2-13.
- Thurber, R. V., Mydlarz, L. D., Brandt, M., Harvell, D., Weil, E., Raymundo, L., Willis, B. L., Langevin, S., Tracy, A. M., Ritchie, K. B., Vega Thurber, R., Mydlarz, L. D., Brandt, M., Harvell, D., Weil, E., Raymundo, L., Willis, B. L., Langevin, S., Tracy, A. M., ... Lamb, J. (2020). Deciphering coral disease dynamics: Integrating host, microbiome, and the changing environment. *Frontiers in Ecology and Evolution*, 8, 575927. <https://doi.org/10.3389/fevo.2020.575927>
- Taylor-Knowles, N., Baker, A. C., Beavers, K. M., Garg, N., Guyon, J. R., Hawthorn, A., MacKnight, N. J., Media, M., Mydlarz, L. D., Peters, E. C., Stewart, J. M., Studivan, M. S., & Voss, J. D. (2022). Advances in immunity 'omics in response to coral disease outbreaks. *Frontiers in Marine Science*, 9, 952199. <https://doi.org/10.3389/fmars.2022.952199>
- Taylor-Knowles, N., Connelly, M. T., Young, B. D., Eaton, K., Muller, E. M., Paul, V. J., Ushijima, B., DeMerlis, A., Drown, M. K., Goncalves, A., Kron, N., Snyder, G. A., Martin, C., & Rodriguez, K. (2021). Gene expression response to stony coral tissue loss disease transmission in *M. cavernosa* and *O. faveolata* from Florida. *Frontiers in Marine Science*, 8, 681563. <https://doi.org/10.3389/fmars.2021.681563>
- Ushijima, B., Meyer, J. L., Thompson, S., Pitts, K., Marusich, M. F., Tittl, J., Weatherup, E., Reu, J., Wetzel, R., Aeby, G. S., Häse, C. C., & Paul, V. J. (2020). Disease diagnostics and potential coinfections by *Vibrio corallilyticus* during an ongoing coral disease outbreak in Florida. *Frontiers in Microbiology*, 11, 2682. <https://doi.org/10.3389/fmicb.2020.569354>

- Veglia, A. J., Beavers, K., Buren, E. W. V., Meiling, S. S., Muller, E. M., Smith, T. B., Holstein, D. M., Apprill, A., Brandt, M. E., Mydlarz, L. D., & Correa, A. M. S. (2022). Alphaflexivirus genomes in stony coral tissue loss disease-affected, disease-exposed, and disease-unexposed coral colonies in the U.S. Virgin Islands. *Microbiology Resource Announcements*, 11, e0119921. <https://doi.org/10.1128/MRA.01199-21>
- Vollmer, S. V., & Kline, D. I. (2008). Natural disease resistance in threatened staghorn corals. *PLoS One*, 3(11), e3718. <https://doi.org/10.1371/journal.pone.0003718>
- Voolstra, C. R., Schwarz, J. A., Schnetzer, J., Sunagawa, S., Desalvo, M. K., Szmant, A. M., Coffroth, M. A., & Medina, M. (2009). The host transcriptome remains unaltered during the establishment of coral-algal symbioses. *Molecular Ecology*, 18, 1823–1833. <https://doi.org/10.1111/j.1365-294X.2009.04167.x>
- Walker, B. K., Turner, N. R., Noren, H. K. G., Buckley, S. F., & Pitts, K. A. (2021). Optimizing stony coral tissue loss disease (SCTLD) intervention treatments on *Montastraea cavernosa* in an endemic zone. *Frontiers in Marine Science*, 8, 666224. <https://doi.org/10.3389/fmars.2021.666224>
- Walton, C. J., Hayes, N. K., & Gilliam, D. S. (2018). Impacts of a regional, multi-year, multi-species coral disease outbreak in Southeast Florida. *Frontiers in Marine Science*, 5, 323. <https://doi.org/10.3389/fmars.2018.00323>
- Wang, P., Bouwman, F. G., & Mariman, E. C. M. (2009). Generally detected proteins in comparative proteomics—A matter of cellular stress response? *Proteomics*, 9, 2955–2966. <https://doi.org/10.1002/pmic.200800826>
- Ward, J. R. (2007). Within-colony variation in inducibility of coral disease resistance. *Journal of Experimental Marine Biology and Ecology*, 352(2), 371–377. <https://doi.org/10.1016/j.jembe.2007.08.014>
- Williams, A., Pathmanathan, J. S., Stephens, T. G., Su, X., Chiles, E. N., Conetta, D., Putnam, H. M., & Bhattacharya, D. (2021). Multi-omic characterization of the thermal stress phenotype in the stony coral *Montipora capitata*. *PeerJ*, 9, e12335. <https://doi.org/10.7717/peerj.12335>
- Williams, L. M., Fuess, L. E., Brennan, J. J., Mansfield, K. M., Salas-Rodriguez, E., Welsh, J., Awtry, J., Banic, S., Chacko, C., Chezian, A., Dowers, D., Estrada, F., Hsieh, Y.-H., Kang, J., Li, W., Malchiodi, Z., Malinowski, J., Matuszak, S., McTigue, T., ... Gilmore, T. D. (2018). A conserved Toll-like receptor-to-NF- κ B signaling pathway in the endangered coral *Orbicella faveolata*. *Developmental & Comparative Immunology*, 79, 128–136. <https://doi.org/10.1016/j.dci.2017.10.016>
- Work, T. M., Weatherby, T. M., Landsberg, J. H., Kiryu, Y., Cook, S. M., & Peters, E. C. (2021). Viral-like particles are associated with endosymbiont pathology in Florida corals affected by stony coral tissue loss disease. *Frontiers in Marine Science*, 8, 750658. <https://doi.org/10.3389/fmars.2021.750658>
- Wright, R. M., Aglyamova, G. V., Meyer, E., & Matz, M. V. (2015). Gene expression associated with white syndromes in a reef building coral, *Acropora hyacinthus*. *BMC Genomics*, 16, 371. <https://doi.org/10.1186/s12864-015-1540-2>
- Yoshioka, Y., Yamashita, H., Suzuki, G., & Shinzato, C. (2022). Larval transcriptomic responses of a stony coral, *Acropora tenuis*, during initial contact with the native symbiont, *Symbiodinium microadriaticum*. *Scientific Reports*, 12(1), 2854. <https://doi.org/10.1038/s41598-022-06822-3>
- Young, B. D., Serrano, X. M., Rosales, S. M., Miller, M. W., Williams, D., & Taylor-Knowles, N. (2020). Innate immune gene expression in *Acropora palmata* is consistent despite variance in yearly disease events. *PLoS One*, 15, e0228514. <https://doi.org/10.1371/journal.pone.0228514>

SUPPORTING INFORMATION

Additional supporting information can be found online in the Supporting Information section at the end of this article.

How to cite this article: Studivan, M. S., Eckert, R. J., Shilling, E., Soderberg, N., Enochs, I. C., & Voss, J. D. (2023). Stony coral tissue loss disease intervention with amoxicillin leads to a reversal of disease-modulated gene expression pathways. *Molecular Ecology*, 00, 1–20. <https://doi.org/10.1111/mec.17110>